General Disclaimer

One or more of the Following Statements may affect this Document

- This document has been reproduced from the best copy furnished by the organizational source. It is being released in the interest of making available as much information as possible.

- This document may contain data, which exceeds the sheet parameters. It was furnished in this condition by the organizational source and is the best copy available.

- This document may contain tone-on-tone or color graphs, charts and/or pictures, which have been reproduced in black and white.

- This document is paginated as submitted by the original source.

- Portions of this document are not fully legible due to the historical nature of some of the material. However, it is the best reproduction available from the original submission.

(NASA-TM-75289) THE EFFECT OF LOAD IN A CONTACT WITH BOUNDARY LUBRICATION (National Aeronautics and Space Administration) 91 p HC A05/MF A01 CSCL 20K

N78-27430

Unclas
G3/37 25848

EFFECT OF THE LOAD IN A CONTACT WITH BOUNDARY LUBRICATION

Introduction

/1*

Boundary Lubrication and Tribologic Test

Let us consider the case of a rotor mounted on an axle supported by two plain bearings. The axle is terminated at each end by a cylindrical swivel pin which turns inside the bore (a sleeve is attached called a bearing bush).

Experiments show that for pressure values used industrially (for example, from 0.1 to 1 decaN/mm^2), it is impossible to turn this rotor at 1500 or 3000 revolutions per minute with rectified tempered steel swivel pins and bearing bushes made of bronze, dry, that is to say, without using a liquid or solid lubricant on the surfaces themselves. The coefficient of elevated friction (for example, from 0.3 to 0.8) produces serious abrasion and seizing.

If one has put oil in each bearing at the start, this can last for a long time, by capillary attraction (several hours) and one can state:

- that the coefficient of friction is very low (for example 0.01).
- that after a period of grinding, the friction of the bearings is negligible.
- that functioning is reliable as long as one maintains the oil in the bearings.

One knows that one can find a parallel case in a state of hydrodynamic support, and that a film of oil which is as thick in its liquid state will undoubtedly surround all the parts of the swivel pins, also preventing them from coming into contact directly, solid on solid, with the bearing bushes.

But, if one decreases the speed of rotation to a very low value, in such a way that the effects of hydrodynamic lift become negligible, one can state that if the coefficient of friction increases, it lasts as long at a value slightly higher than the value obtained dry. In these conditions the friction coefficient is approximately between 0.1 and 0.2. One also observes that if wear of the bearings is not zero, however it is low and regular.

---

*Numbers in the margin indicate pagination in the foreign text.

One must interpret the phenomenon considering that if there is any liquid which continues not to be inserted between the pin and the bearing bush, it remains between the lubricant molecules, probably in an extremely thin layer which considerably modifies the phenomena of friction between the two surfaces.

A completely identical phenomenon is observed systematically in the movements of machine tool carts or tables. The manually operated movements, with a crank controlling an endless groove, can be very slow, the force used corresponding however to the low value of the friction coefficient even when no phenomenon of hydrodynamic support can be involved.

In preceding examples, reduction of the friction coefficient due to action (hypothetical) of superficial films of organic molecules is a result of the boundary lubrication phenomenon.

Perhaps this phenomenon can be shown by laboratory experiments carried out on a tribometer (friction machine).

If one immerses a sample in a solution of polar molecules in a solvent with very low concentration, the molecules are adsorbed on the metal surface. The sample will also, once it has been removed from the solution, be covered with a lubricant film deposited by adsorption. If the coefficient of friction obtained dry after cleaning the samples is on the order of 0.5, for example, it drops toward 0.1 when the tests are carried out after this boundary lubrication film has been deposited by adsorption. Microscopic observation after the friction shows the existence of fine stripes and wear on the test samples.

This simple experiment shows the two aspects of boundary lubrication:

- physical and chemical aspect (adsorbed polar film) /2
- mechanical aspects (deformation of the body on contact)

Duringthe friction tests, it is necessary to understand perfectly the parameters which define this boundary lubricating contact:

- tribologic data: load applied, slip speed.
- contact geometry.
- microgeometry of the samples (roughness).
- metallurgical characteristics of these samples (composition, durability...)

- physical and chemical nature of the adsorbed film (rate of recovery of the surface expressed in the number of equivalent adsorbed monofilms).

- conditions of cleanliness and precision of experimentation.

We have placed ourselves in particular tribological conditions:

- the tests were carried out with increasing load.

- the contact is of the hemispheric small plate rubbing contact type. This contact has the advantage of being known from a mechanical point of view (distribution constraints, deformations).

- A single weak pass, with increasing load, of the friction piece on the plate is carried out. The friction piece also encounters throughout the test a surface untouched by friction. We can also study variations in the load function of interface behavior without being constrained by chemical transformations of the film deposited which could appear during alternative friction coming and going from rubbing contact on the small plate.

- friction is carried out at low speed (0.01 mm/s).

- the rate of variation of the load is low.

These tribological conditions being chosen, the object of this experimental work has been to separate the different factors affecting the behavior of the interface induced in the boundary procedure. We have attempted to quali tatively determine the relative effect and the direction of variation of various parameters which define the boundary lubr cated contact.

Experimental Material /3

Tribometer

This test machine of the hemispheric friction type on a plane is shown in figure 1. The hemispheric friction piece F is located at the end of arm B acting like a balance, being able to pivot in a vertical plane around the A axle. This A axle is solid in frame C fixed at the end of flexible sheets.

When the friction piece is subjected to a friction force, the latter is in a direction perpendicular to the axis of arm B and involves flexion of the sheets. A dynamometer ring a1 makes it possible to measure displacement of the frame C and to evaluate the force of friction after calibration.

The increase in load during displacement is realized when filling receptacle V and is controlled by the dynamometer ring a2.

A slow speed motor requires displacement of the micrometer table on which the small plate P is fixed.

The characteristics of the tribometer are:

- field of 0-50N load
- displacement velocity, 0.01 mm/s
- rate of load increase $5 \cdot 10^{-2}$N/s
- course of the friction piece on the small plate, 10 mm.

The equivalent hertz pressures in this load field will be by smooth ball bearing contact (6 mm radius) -- a smooth plane, 0-110 kg/mm^2.

During the friction, the development of the friction coefficient and electrical resistance from contact between the friction piece and the small plate are recorded. The diagram of measurement of electrical resistance from contact is shown in figure 2. A digital voltmeter makes it possible to observe the difference in the potential produced between the friction piece and the plate by a current source maintained at 10 mA.

The tribometer is placed on an antivibration table. The tests are carried out in a white, dust-free room; the temperature is constant at 20°C ± 1°C, humidity is 45% ± 5%.

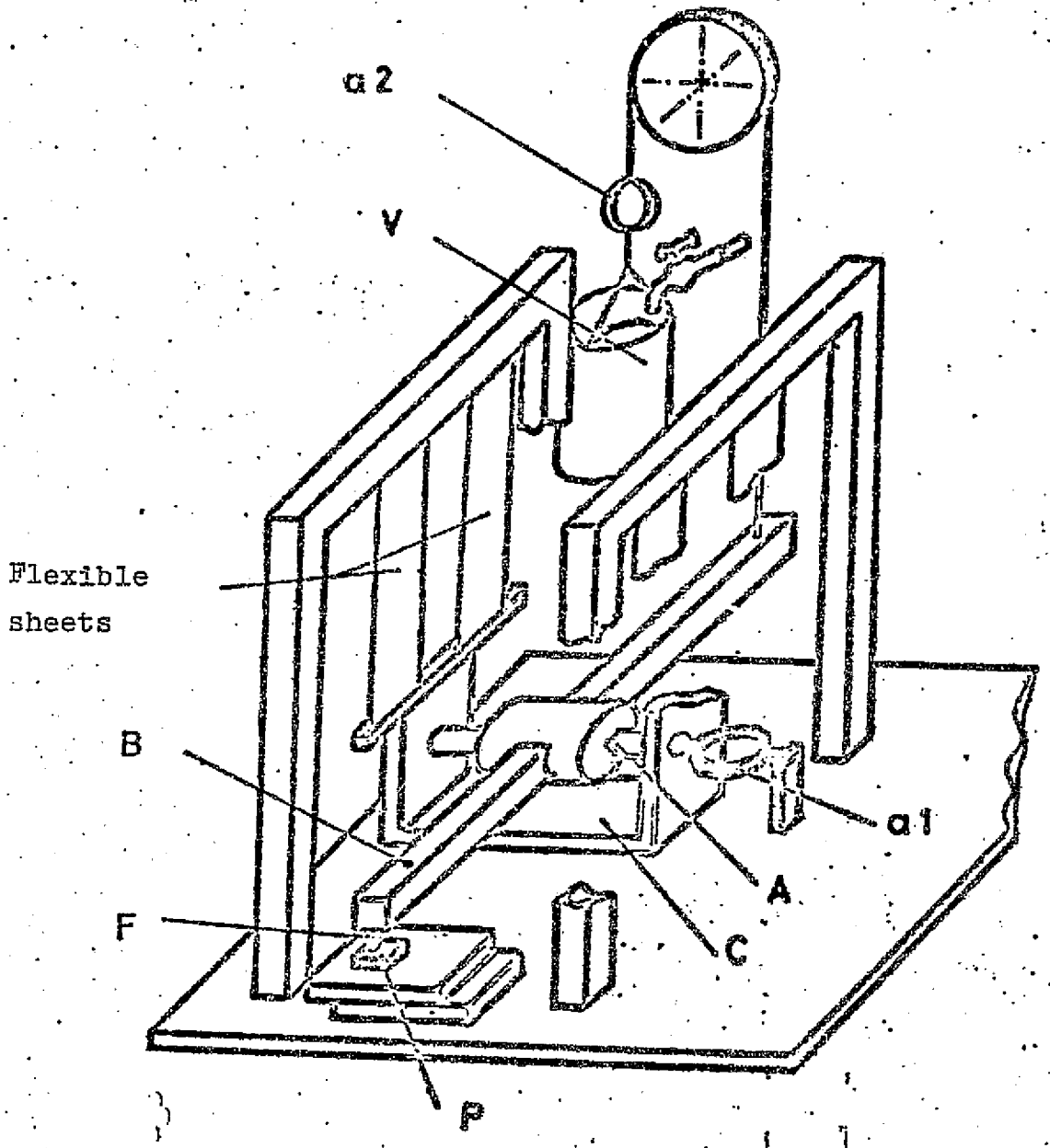

FIGURE 1

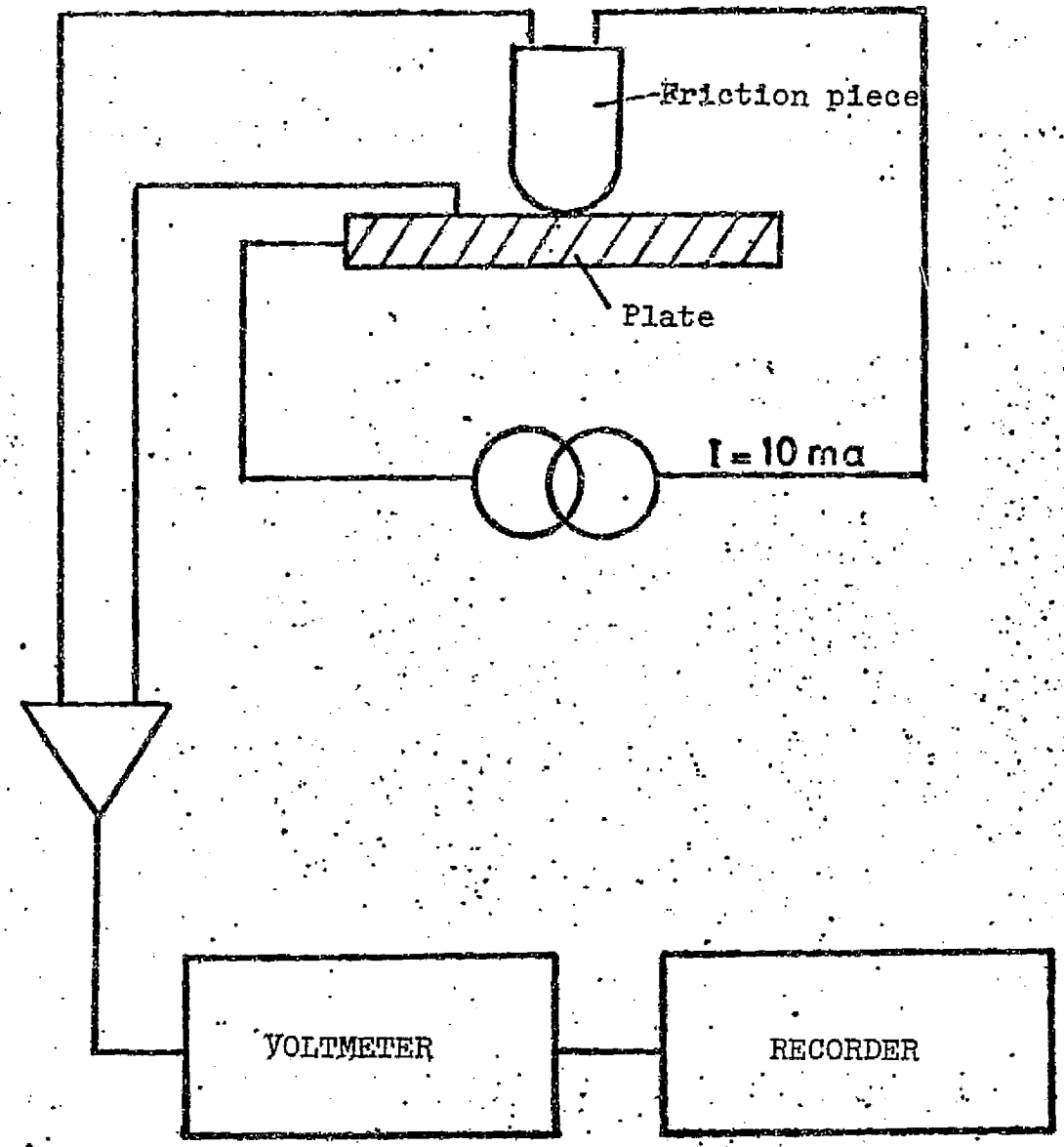

FIGURE 2

Samples Tested

Friction pieces: two types of friction pieces were used --
- hemispheric friction pieces with radius of curvature 6 mm in a cobalt based alloy (51% Co, 30% Cr, 13% W, 2.3% C). Hardness is 850 Hv.
- ball bearings with different curvature radii of 100 C6 steel. Hardness 900 Hv.

These friction pieces are diamond polished 1 μm, their roughness being on the order of 0.02 μm (RMS).

Plates: two types of small plates were used --
- plates made of a cobalt base alloy (60% Co, 27% Cr, 5% W, 2% C) of different roughnesses obtained by the following procedures:
  - granulation to file dust
  - sanding to sand
  - microball test with glass balls
  - microball test on aluminum
  - grinding
  - diamond polishing at 1 μm

These plates have the following mechanical characteristics: Hv = 610 kg/mm^2; E = $26 \cdot 10^3$ kg/mm^2
- plates of cobalt block (99.9%) diamond polished at 1 μm (roughness RMS = 0.05 μm). Hardness Hv = 400 kg/mm^2.

Method of Determining the States of the Surface of these Samples

We have used a statistical analysis of these surface states adopting the Greenwood and Williamson [1], Whitehouse and Archard [2] models. The parameters which characterize the different sandings and other surfaces are:

- type σ variation of distribution of the heights of the peaks of asperities. /6

- the mean β curvature radius of the peaks of asperities.

- the N number of asperities per unit of surface.

These parameters were obtained by a method of statistical and frequency analysis realized in real time.

The models cited above and the operator method are recorded in appendix A.

Cleaning and Lubrication Films Tested.

- cleaning: the "degree of cleanliness" of the samples before lubrication is an important parameter. A very small quantity of adsorbed polar molecules suffices, in effect, to influence the friction results. In theory, one calls the surface "clean" if it is a surface free of all molecules foreign to this solid. But, obtaining such surfaces is practically impossible. Consequently, for this study, we will consider that the surface is "clean" when it is contaminated in a reproducible controlled fashion, the foreign molecules which exist not being more than slightly adsorbed (in this case, the friction coefficient is elevated).

A systematic study of the range of cleanliness has been made previously at a laboratory putting different energies into play (mechanical, caloric, chemical), in order to obtain desorption of molecules firmly fixed on the surface.

The best result, also confirmed by friction tests without a lubricant, has been obtained by the cleaning cycle used for this study.

This cycle comprises:
- ultrasonic baths in acetone for analysis
- extraction of the Soxhlet type (acetone for analysis)
- discharge in a vacuum

- lubrication films:

Different lubrication films were used: a monolayer of stearic acid deposited by the following method: immersion of the sample in a solution of stearic acid solvent (hexane or cyclohexane) in a concentration of 10^{-4} g/cm^3. After a certain time (20 min to 1 hr), the sample was withdrawn slowly from the solution. This time makes it possible to adsorb the polar molecules of the fatty acid on the surface. Inspection by radiotracers (total counting of the labeled molecules) verifies the reproducibility of the adsorbed film. The films obtained also correspond to about the equivalent of a uniform adsorbed monofilm. The tests carried out in the laboratory have shown that this monofilm is not uniformly attached to the solid, the separation of the fatty acid on the surface makes for small discontinuous "packets" [3].

Some tests were carried out without removing the samples from the solution. The results were identical to those obtained on samples removed from the deposit solution after adsorption.

- film of solvent only, the tests were carried out with samples immersed or removed from the solvent (in these two cases, the results were similar).

- stearic acid film obtained by immersion then contraction following polishing with cloth (the film obtained corresponds to an equivalent of 0.4 monofilm).

- in order to visualize the phenomenon, an insulating film of varnish diluted in acetone was used.

PART 1

PHYSICAL AND CHEMICAL ASPECT OF CONTACT SHOWN BY TRANSITION LOADS

1.1. Transition Loads Shown

1.1.1. Experimental Conditions

- A monolayer film of stearic acid.
- Plate: material: cobalt base alloy. This plate is polished and has the following parameters of roughness:

  $\sigma = 0.05 \pm 0.02$ µm
  $\beta = 50 \pm 2$ µm

- Friction piece: cobalt base alloy having almost the same roughness as the plate.

  Curvature radius: 6 mm

- Test carried out with increasing load: 0-50 N
- Rate of load increase.: $5 \cdot 10^{-2}$ N/s
- Rate of displacement of the friction pieces in relation to the plate: 0.01 mm/s
- During the test, the friction coefficient and the electrical resistance of the contact were recorded.
- After the test, microscopic observation of the friction trace was carried out.

1.1.2. Results and observations

Figure 1.1. shows the development of the friction coefficient, electrical resistance of the contact and breakdown of the surface of the plate during this test at increasing load.

- Friction Coefficients µ:

Between the zero load (beginning of the test) and a certain load W_A, the friction coefficient remains constant and does not fluctuate. Between this load W_A and a load W_B which is higher, slight fluctuations are apparent. Below this latter load W_B, µ oscillates strongly. This corresponds to part of the relaxation oscillations (Stick Slip) and to enormous fluctuations. These oscillations, as has been shown elsewhere [4]

FIGURE 1.1

Film: stearic acid
Polished plate

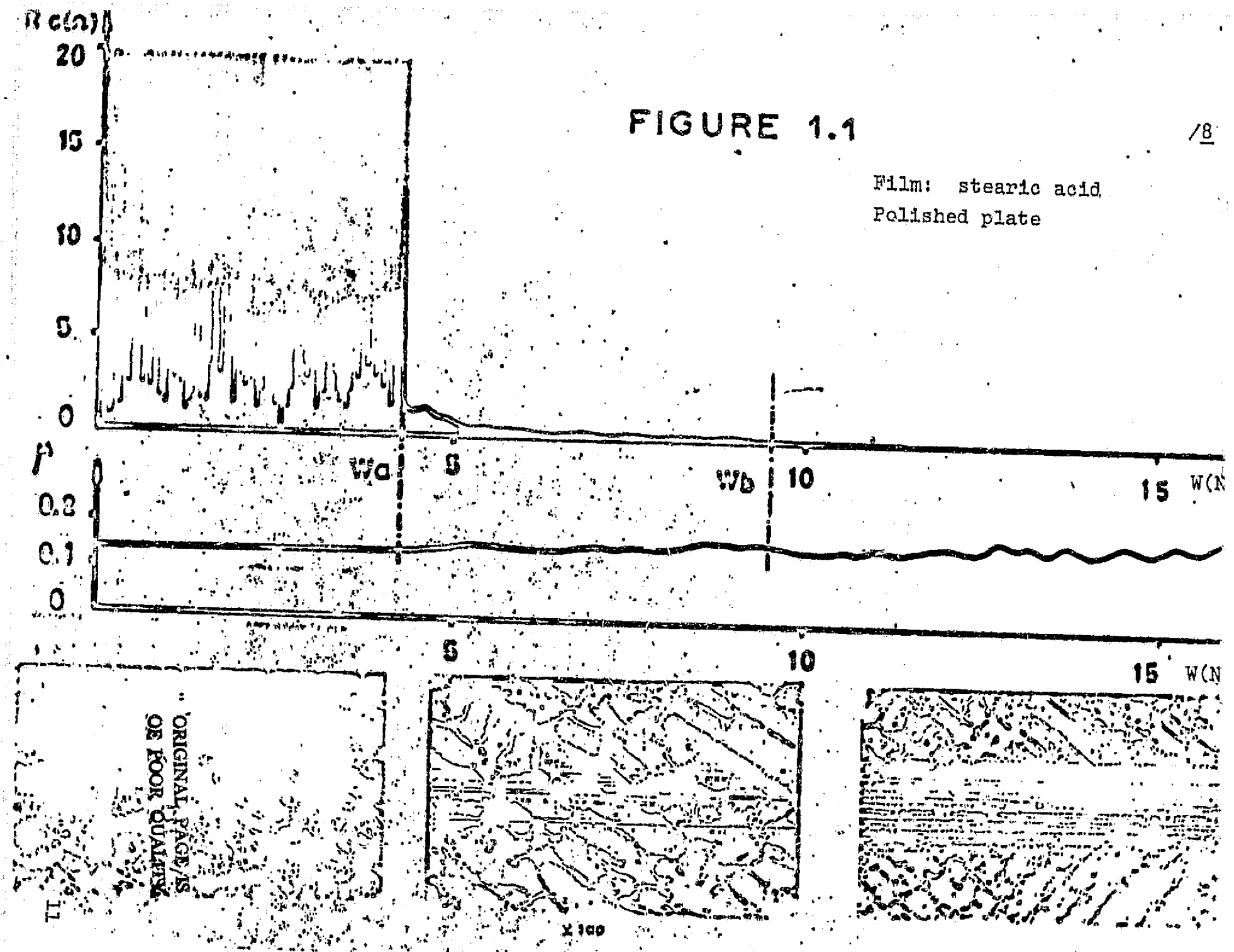

are not due uniquely to friction conditions of the interface but also depend on the mechanical characteristics of the tribometer (rigidity of the elastic sheet system).

- Electrical Resistance of the Contact Rc:

Simultaneously, between the zero charge and W_A, the value of electrical resistance oscillates with high amplitude and frequency. The mean value is several ohms. The voltage is on the order of several dozens of millivolts (20 to 50 mV). These low voltages minimize the possibility of electrical discharge in the contact which causes rupture and breakdown of the boundary film [5]. Between W_A and W_B, the fluctuations have a weaker amplitude and frequency. The mean value of electrical resistance is several tens of ohms and decreases slowly toward zero as the load increases. Below W_B electrical resistance is practically zero.

- Development of Contact Deterioration /9

Examination of the friction tracing shows that before W_A, contact deformation is of a "fresh" type: the deformation, even if the boundary film is insulated from the point of view of the electrical contact between the friction piece and the plate, prevents close microcontacts between solid and solid. The scratch left on the plate has an elastic aspect without lifting. The deformation is "severe" (lifting) after W_A.

1.1.3. Bibliographical Note

A similar experiment has been carried out by Hirst, Kerridge and Lancaster [6]. These authors have shown by a tribologic test at increasing load, the existence of two transition loads. For the type of contact given, a film and a roughness of the surface given, the amplitude of variations of the friction coefficient instantly develop when the load increases. They showed by contact radiography that above the first load W_A, the first metal transfers appear from the radioactive friction piece on to the plate. Above the second load W_B, these transfers are important and the contact is very damaging (figure 1.2).

1.1.4. Conclusion

- Two transition loads W_A and W_B can be used as evidence for friction tests with increasing load.

- The W_A load is characteristic of a clear evolution in the contact, namely, passage from a mode of "fresh" friction to a mode of destructive friction.

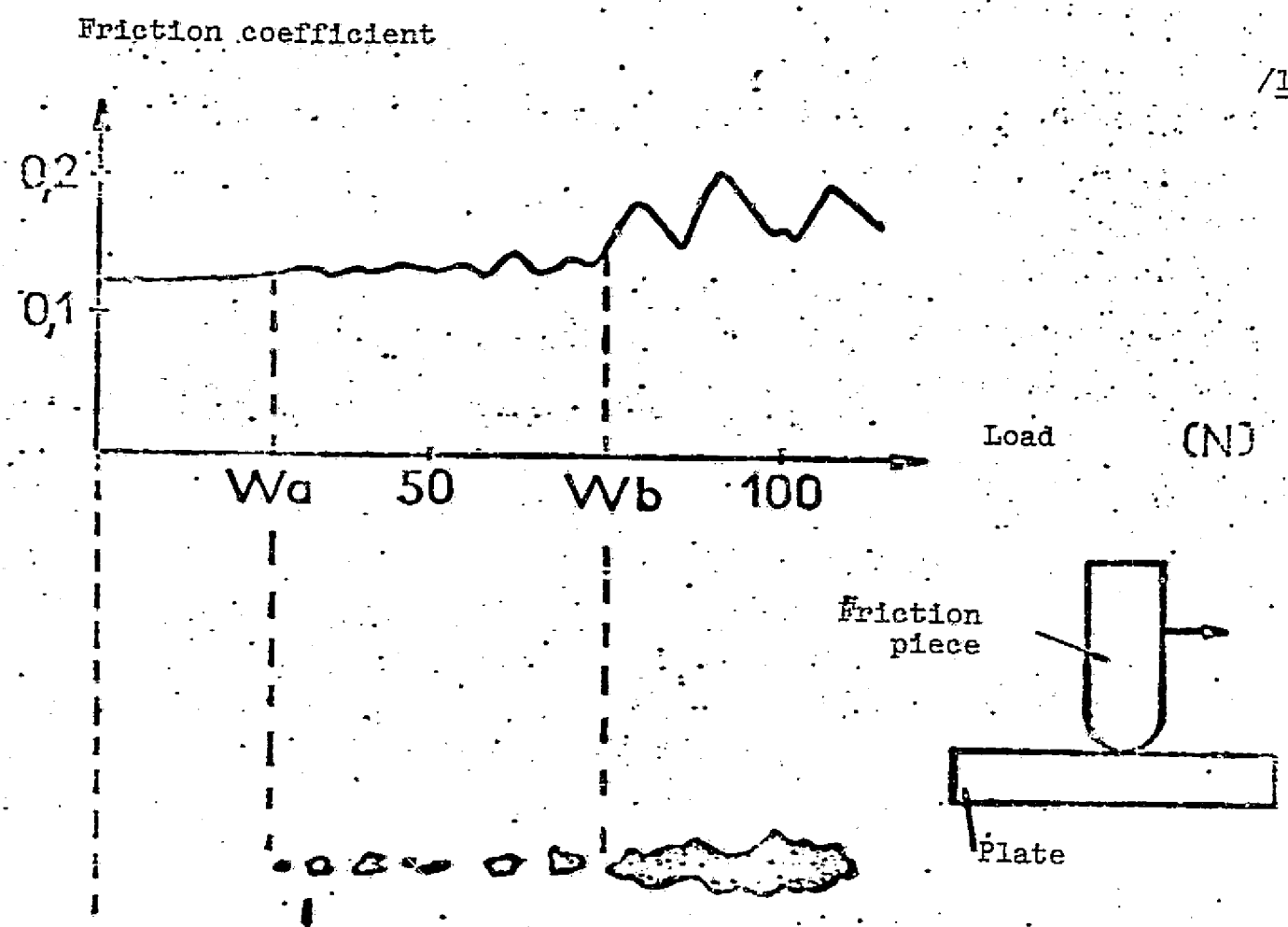

Friction piece: copper Ø9 mm

Plate: copper

Film: stearic acid

FIGURE 1.2

This transition is manifested by:

- The appearance of serious scratches
- The appearance of transfers [6]
- Relaxation oscillation of the friction coefficient (which depends on the tribometer used).
- The drop in the mean value of electrical contact resistance.

- The W_A shows the end of the lubrication role of the deposited boundary film. Following this explanation, we will interest ourselves in the effect of various contact parameters on this load W_A.

1.2. Effect of the Lubricant Film

1.2.1. Experimental Conditions

Two series of experiments have been carried out:
First series: The metal samples were the same as those described in the preceding test (friction pieces and polished small plates), and different deposited lubricating films were tested on the plates.

a) ASM: stearic acid film deposited by immersion, the sample being withdrawn from the deposit solution after immersion (1 monolayer).

b) ASB: stearic acid film deposited by immersion, the test being carried out when the sample is immersed again in the deposition solution.

c) ASMC: stearic acid film deposited by immersion then removal and subsequent polishing with a cloth (0.4 monolayers).

d) CM: cyclohexane film, the test being carried out after evaporation of the solvent.

e) CB: cyclohexane film, the test being carried out while the sample is immersed in the solvent.

f) Dry: without lubricating film, the plate is tested following the cleaning cycle.

Second series: After being sanded, the plates (the parameters /11 of this roughness are $\sigma = 0.42 \pm 0.02$ µm $\beta = 26 \pm 2$ µm), were tested with four boundary lubricating films.

a) ASM: stearic acid film deposited by immersion then removal (about 1 monolayer).

b) ASB: stearic acid film, the test being carried out when the plate is immersed in the deposition solution.

c) CM: cyclohexane film.

d) Dry: without lubricating film, the plate having completed the cleaning cycle.

1.2.2. Results

The loads W_A obtained during these two series of tests, for different films studied, are recorded in the tables below. More experiments were carried out in each case and the values of the loads are the mean values obtained.

Series 1

Smooth friction pieces
Smooth plates

Film	ASM	ASB	ASMC	CM	CB	DRY
W_a(N)	5,5	5,5	>50	3,5	3,5	0

Series 2

Smooth friction pieces
Rough plates

Film	ASM	ASB	CM	DRY
W_a(N)	3	3	1,5	0

The polished plates used in the first series of tests make it possible to make microscopic observations of the friction traces. As has already been shown, for the ASM film (figure 1.1.), before W_A, the contact deformation is of the "fresh" type (the scratch has an elastic aspect), the deformation being severe (lifting) after W_A. For the ASMC film (figure 1.3) where W_A is not apparent, the deformation remains "fresh" in the entire field of the load studied (depressions of an elastic type). During the Dry test (figure 1.4), the sample coming from the cleaning cycle, where W_A appears from the contact, severe scratches and the lifting are present all along the test piece.

1.3. Interpretation

1) The W_A loads obtained on the stearic acid films deposited by immersion then removed are the same as those obtained on adsorbed stearic acid film when the test is carried out with the plate always immersed in the deposition solution (first series of tests: ASM and ASB films, second series of tests: ASM and ASB films). It is known [8] that if one immerses a piece into a solution of stearic acid and solvent, there is produced preferential adsorption of the stearic acid resulting, after a certain time, in complete covering of the surface. If the solvent is such that the surface tension is

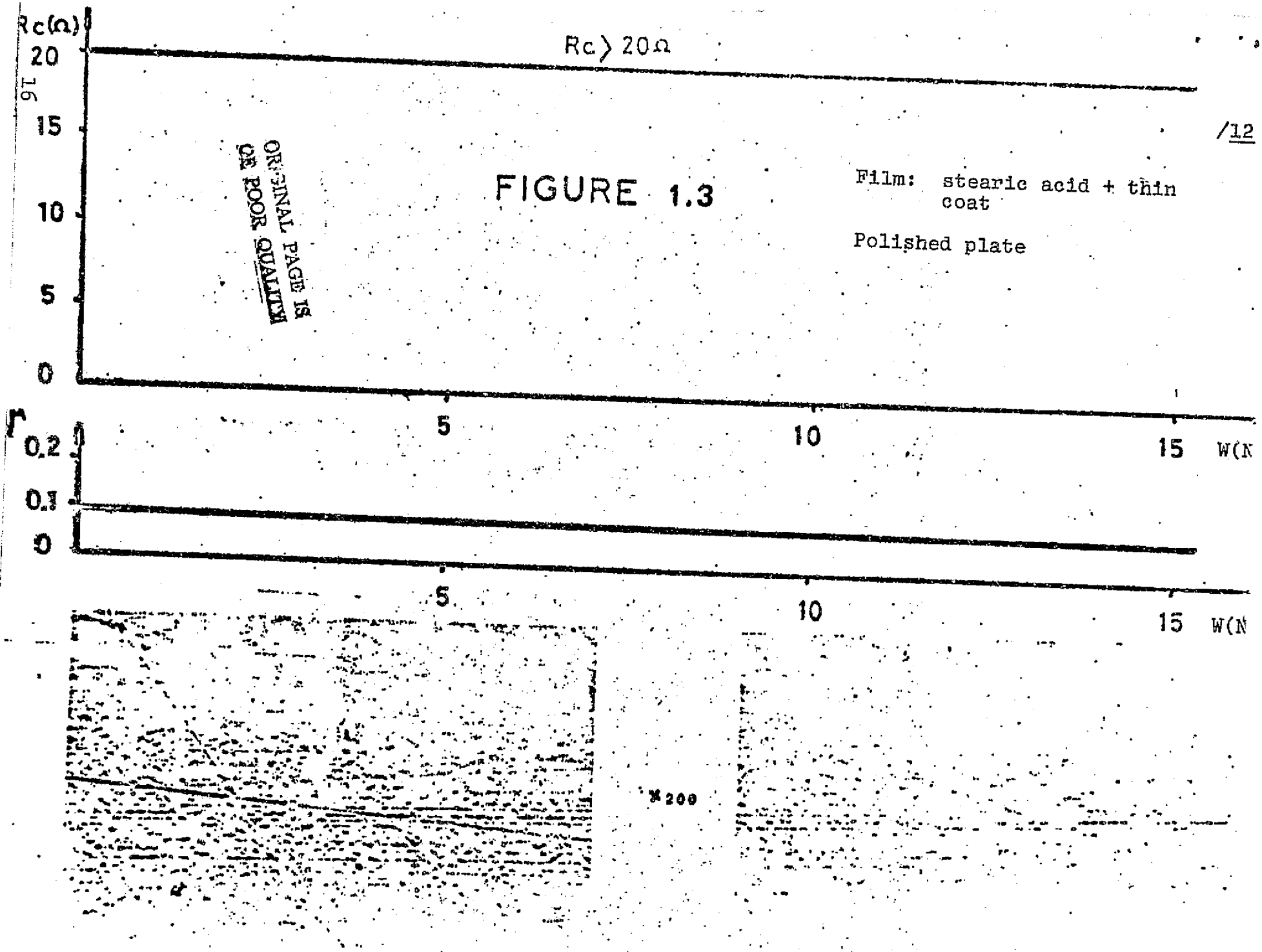

FIGURE 1.3

Film: stearic acid + thin coat

Polished plate

FIGURE 1.4

Without deposited film /13

Polished plate

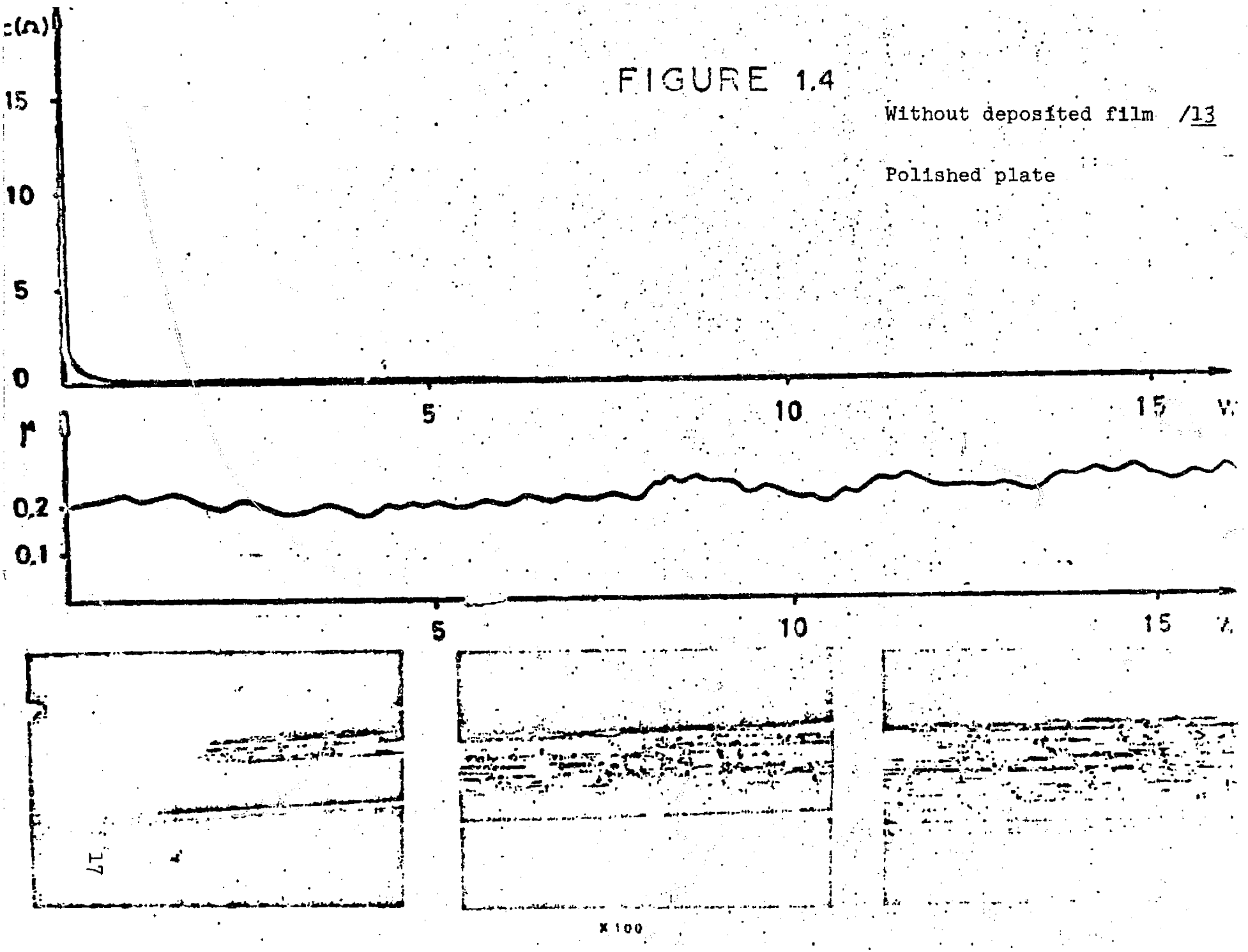

higher than the critical surface tension γc of the film, then with removal, the solution does not wet the surface on which /14 the film is adsorbed. In this case (which is one of the stearic acid-cyclohexane solutions), wetting [8] makes it possible to say that the film has formed on the metal surface.

The friction tests carried out in ASM or ASB conditions are identical and there is a high possibility that these lubricating boundary films are identical.

2) The adsorbed stearic acid film on the surface is more favorable for friction than the solvent film alone: in effect, it is known that the molecules of organic compounds contain a polar group sticking better to the oxidized metal surface than those of a nonpolar solvent [8]. On the other hand, it has been shown [9] that polishing with a cloth improves the boundary friction. This rubbing lifts a part of the deposited film (the equivalent of a monolayer of film is 0.4 when it was 1 before the rubbing). But it seems that during this procedure, the molecules which are not removed cling more strongly to the surface [10]. The efficiency of these films was well known: the friction coefficient and wear are, at a given load, weaker with a film which has been subjected to rubbing than with a film without rubbing. This has proven to be a very strong influence on the transition load Wa.

3) The Wa load is weaker for a cyclohexane film than for a monolayer of stearic acid. This result seems logical as one knows that cyclohexane is a poor lubricant. The point which is always surprising is that the difference between ASM and CM or ASB and CB is not clearer. It is very possible that impurities are present in low proportion in the product which, however, is very pure and realizes an adsorbed film on the surfaces.

4) Examination of the friction traces (on the polished plates of the first test series) has shown that Wa, and the rupture load of the film in the interface coincide with the appearance of severe scratching and lifting. This is not to say that before Wa there were not any scratches but, as has been shown, Wa marks an evolution in the appearance of the deterioration of the surface: scratches of a "fresh" aspect before Wa, lifting after Wa.

5) For the same boundary film tested, the Wa load is lower than for a polished plate.

(First series ASM film, second series, ASM film).

These statements show that the mechanical aspect of boundary lubrication is present implicitly in these friction tests.

PART 2 /15

CONTRIBUTION OF MECHANICAL CONSIDERATIONS TO THE STUDY OF RUPTURE OF THE BOUNDARY LUBRICATING FILM

II.1. Introduction

The mechanics of the surfaces is of interest to the contact study. Two types of contact are present:

- static contact
  - at normal load $\vec{W}$ alone
  - at normal load $\vec{W}$ plus tangential force $\vec{T}$
- dynamic contact
  - normal charge $\vec{W}$ plus tangential force $\vec{T}$

At the present time, the models developed have been proposed for a case of static and punctual contact between the polished body:

- Hertz model [11] in the case of an elastic contact.

- hardness model [12] in the case of plastic contact.

The Hertz model was extended to smooth ball bearing contact of the roughness plane by Greenwood and Tripp [13], Appendix A.

In the case of a dynamic contact, some of the deformation models of contact bodies have been proposed (Appendix B).

We will put ourselves in tribological conditions so that the mechanical aspect of contact is as well known as in the preceding models cited, that is to say: polished hemispheric friction piece, polished or rough plate -- Greenwood and Tripp [13] assumethat a rough surface is comprised of N asperities per unit of surface in which the mean curvature radius of the peaks is β and in which the heights follow a Gaussian division of the σ type variation (Appendix). To satisfy this hypothesis as well as possible, the roughness of the plates was obtained by sanding.

II.2. Application of the Contact Models to Samples Used

II.2.1. Static Contact at Normal Load Only

- Let us assume an ideal smooth contact

The end of the elastic field results when mp, mean pressure of contact is equal to 0.4 H, H being the hardness of the material.

$$mp = \frac{W}{A}$$

W -- load

A -- Hertz contact area

$$W = \frac{4}{3} E' \beta^{1/2} \alpha^{3/2}$$ According to Hertz (1)

$$A = n \beta \alpha$$

- β: curvature radius of the friction piece
- α: compliance: bringing together of two points, during contact, these points were removed from the deformation zones.

- E' such that $\frac{1}{E'} = \frac{1-\nu_1^2}{E_1} + \frac{1-\nu_2^2}{E_2}$
- ν_1, ν_2: Poisson coefficients in relation to the ball bearing and to the plane
- E_1, E_2: Young's modulus in respect to the ball bearing in the plane

For the contact study

$E' = 12200$ kg/mm^2 $H = 610$ kg/mm^2 $\beta = 6$ mm

also, at the boundary of elastic deformation $mp = 5178 \frac{\alpha^{1/2}}{\beta^{1/2}} =$ /16

0.4 X 610.

from which α boundary of elastic deformation = $12.8\ 10^{-3}$ mm

Formulas (1) give then W boundary = 57 kg. In the field of load tested, the contact, assumed smooth, will be elastic.

If we take the radius of the circle graphically appearing from contact a as a function of load

- elastic field: $a = (\frac{4}{3} E \beta)^{1/3} W^{1/3}$
- plastic field: $W = AH$ from $a = (\frac{1}{nH})^{1/2} W^{1/2}$

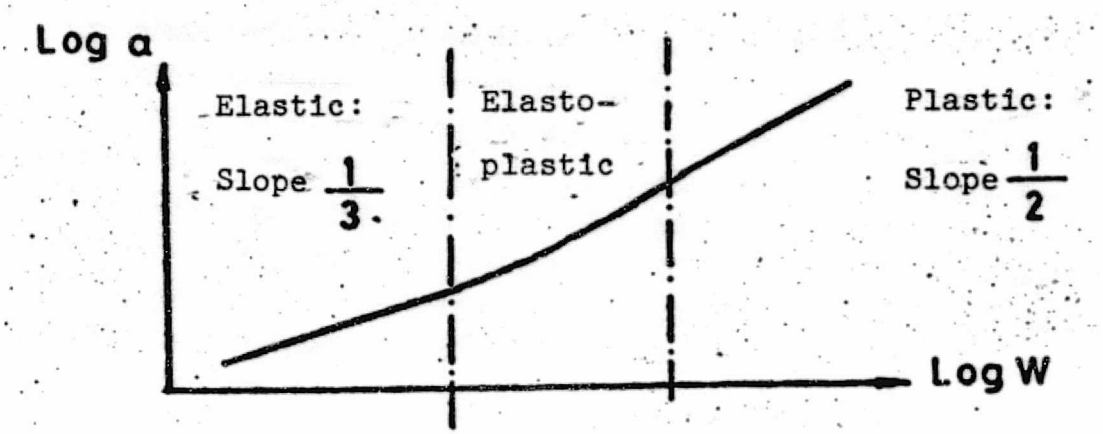

This curve sums up the evolution of static contact as a function of load, the ball bearing and the plate being assumed smooth.

Case of rough samples

- Application of the Greenwood and Tripp model [13], Appendix A, has shown that in the field of loads tested (0, 50 N) the number of asperities in contact was small whichever sample was used.

- on the order of 5 to 8 to 50 N
- on the order of 2 to 3 for W<10 N

For the WA loads (lower than 10 N), as will be shown, the number of contact asperities is on the order of from 2 to 3.

- Let us apply the theories of Hertz contact to contact of an asperity on the friction piece. The curvature radius of the friction piece is assumed to be infinite in relation to that of the asperity.

β of asperity (μm)	α boundary (μm)	W elastic maximum for asperity (N)
44	0,094	3×10^{-6}
26	0,055	$1,1 \times 10^{-6}$
20	0,043	$0,65 \times 10^{-6}$
15	0,032	$0,36 \times 10^{-6}$
6	0,013	$0,06 \times 10^{-6}$

The WA loads vary from 0.6 to 5 N (as will be shown), the 2 or 3 asperities in contact are plasticized.

11.2.2. Dynamic Contact /17

Dynamic motion causes an increase in deformation of the contact surfaces. Figure 2.1. shows a topographic relief of tracings left on the plate at 20 N. The slip which occurs when the plate is loaded at 20 N static causes shearing of the protrusion formed at the front of the friction piece during preliminary motion [14], Appendix B.

11.2.3. Contribution of the Contact Models:

These mechanical models of the surface show that it is necessary to study the following in the boundary lubricated contact:

- effect of slip on contact deformations
- effect of roughness
- effect of hardness of the plate
- effect of the macrogeometry of contact (curvature of the friction pieces is hemispheric, for example).

II.3. Static Test and Dynamic Test

Maintaining the boundary lubricating films must be greatly affected by these deformations of the interface during tangential motion. Some tests at increasing loads similar to that described previously were carried out. Each test with slip of the friction piece in relation to the plate was duplicated by a static test without slip where we were interested in the evolution of electrical resistance from contact as a function of load (figure 2.2.). Figure 2.3. shows the aspects of recording contact resistance Rc as a function of load W for two tests with and without slip made in parallel. The film is a monolayer of ASM stearic acid, the plate is sanded to a roughness parameter of $\sigma = 0.42$ µm $\beta = 26$ µm.

- Test with Slip, Dynamic

Development of electrical contact resistance as a function of load has the same aspect as that described in the first experiment. The WA load appears in these experimental conditions at about 260 gf, the value of the contact resistance oscillates strongly before this load. The interpretation of these fluctuations of Rc for $0 < W < WA$ is not precisely known. It can be suggested [15] that these fluctuations would correspond to "intermittent weaknesses" of the boundary layer caused by the friction.

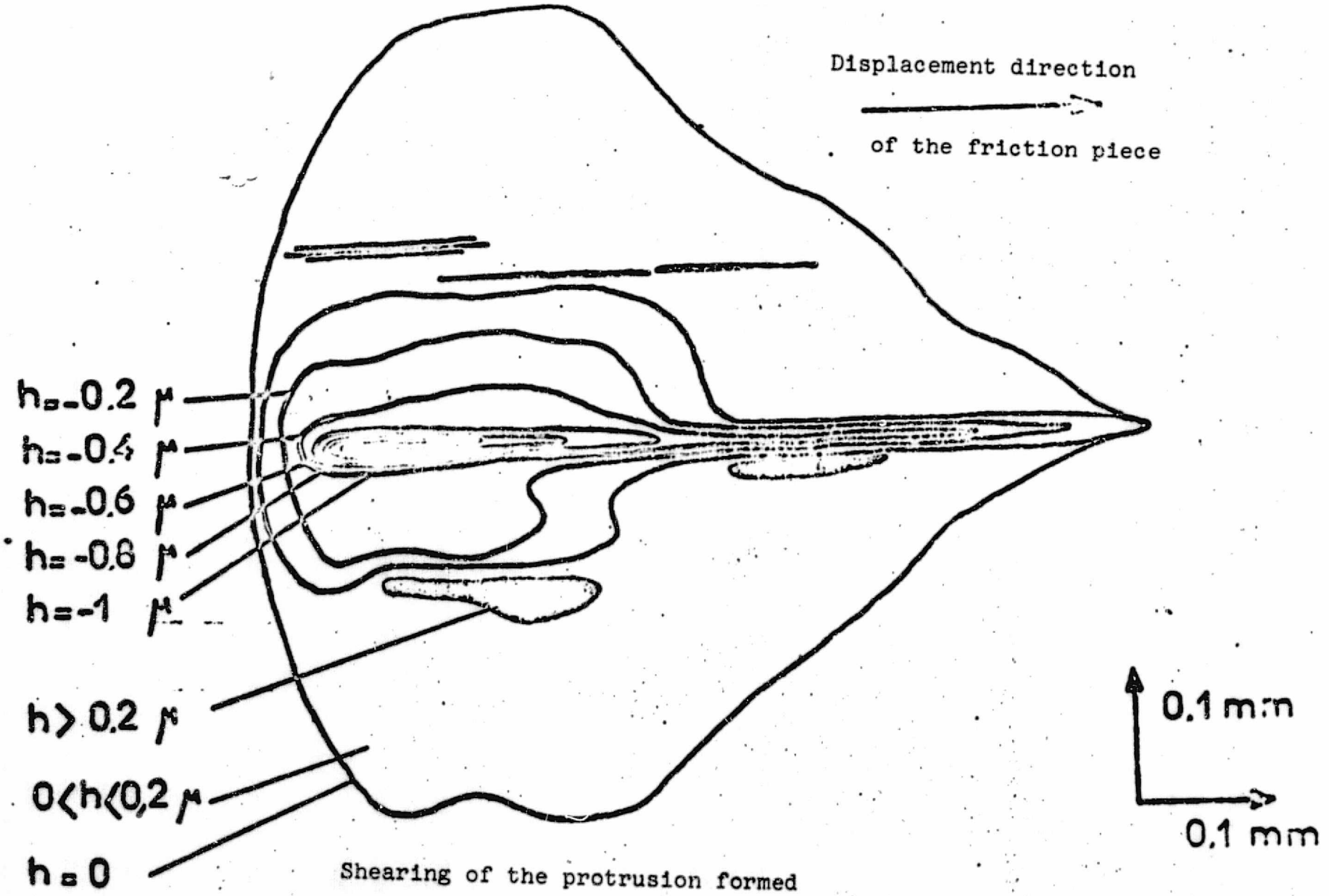

Shearing of the protrusion formed during preliminary motion

FIGURE 2.1

W increasing from 0 to 10 N

1 single pass

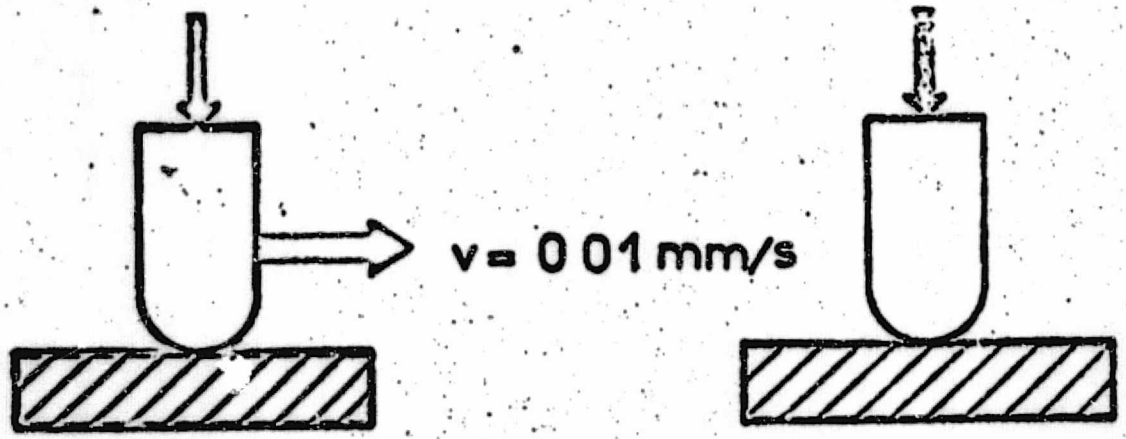

DYNAMIC

W increasing from 0 to 10 N

STATIC

FIGURE 2.2

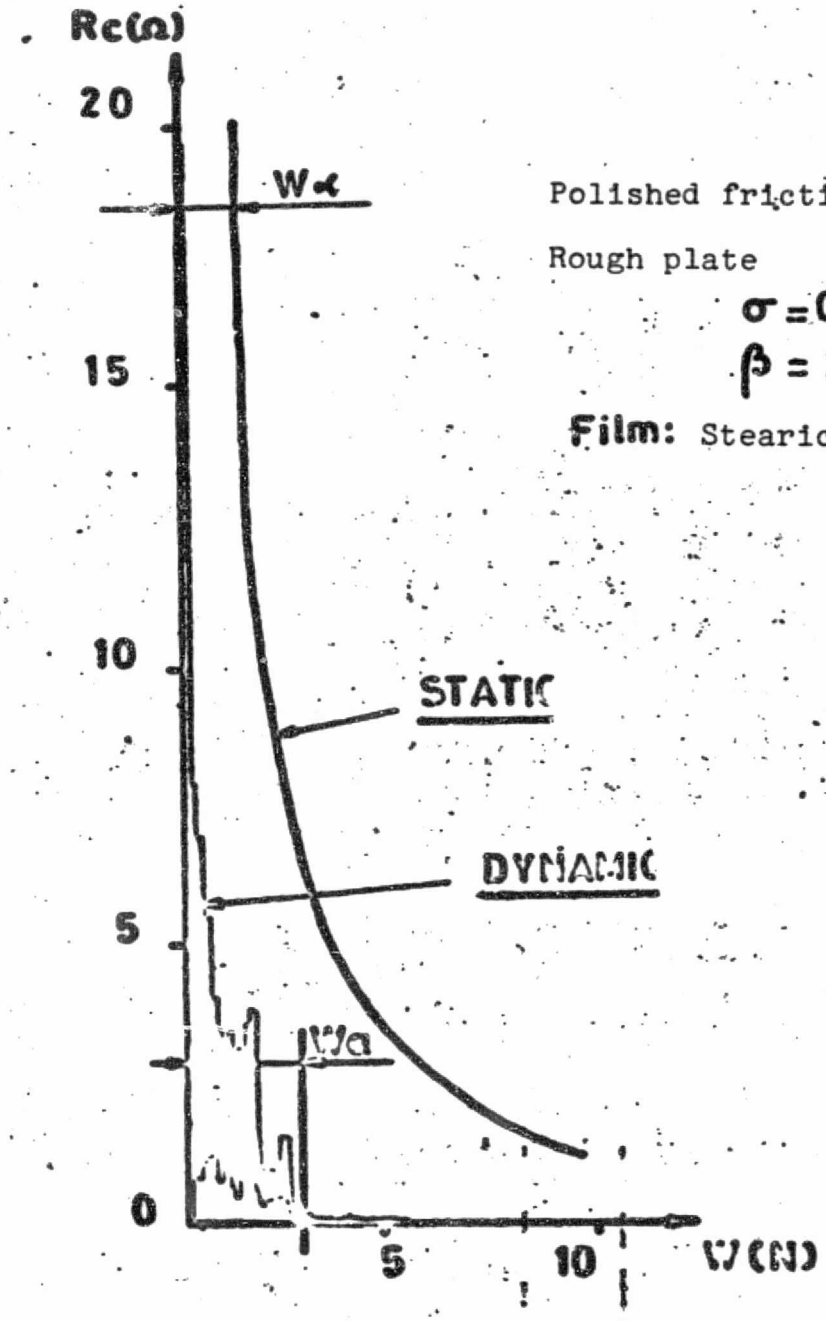
Rc(Ω)
20
15
10
5
0
Wα
STATIC
DYNAMIC
Wa
5
10
W(N)
Polished friction piece
Rough plate
σ = 0,42 μm
β = 26 μm
Film: Stearic acid

FIGURE 2.3

- Static Test Without Slip

Decrease in the value of contact resistance is regular, without oscillations during increase in load. It does not produce electrical rupture of the boundary film in the field of load studied: the lubricating layer can resist very high loads in a static test. This has already been pointed out by Tabor and Willis [15] who have also shown that all vibration or all microdisplacement of friction in relation to the plate can result in rupture of the boundary film. This decrease Rc = f (W) follows the power law in the measurement field (0 - 20 Ω)

$$Rc = \frac{k}{Wn}.$$

In the types of contacts studied, the series $1.5<n<2$ will be discussed. Not wishing to use the technique of electrical contact resistance except as a qualitative means of studying static penetration of the boundary film, we will characterize these decreases by Wa, whose load Rc becomes lower at 20Ω, the upper boundary of our range of measure.

II.4 Rôle of Surface Roughness /21

II.4.1. Experimental Conditions

Tests with and without slip can be carried out on sanded plates as has been previously described. The friction piece is hemispheric with a curvature radius of 6 mm and polished. The boundary film tested corresponds to an equivalent of a monolayer of stearic acid. This test can also be carried out with a ground plate and with polished plates.

- A dozen tests have been carried out on slip for each roughness. The load fields where transition Wa occurs are recorded in the table of results. When the load is higher at Wa, relaxation oscillations appear. The mean value of the friction coefficient μ (the value around which these fluctuations occur) is slightly higher than the value of the coefficient of smooth friction which exists before Wa. These values of μ before Wa and the mean μ after Wa are recorded.

- The static tests without slip can be carried out on four plates: three rough plates and one polished plate. The mean loads Wa for many tests are shown in the figure below (loads at which Rc becomes lower than 20 Ω).

II.4.2. Results

SAMPLE	$\sigma(\mu m)$ $\pm 0,02$	$\beta(\mu m)$ ± 2	N/mm^2 ± 5	μ Smooth $W<W_a$	μ Mean $W>W_a$	W_a (N)	W_α (N)
A	5.79	6	50	0,30	0.30	0,2-0,9	0,6
B	2.05	44	15	0,20	0,27	4,5-5,3	2.5
C	0,76	15	95	0.22	0,26	0.4-1,2	
D	0,44	26	100	0.20	0.26	2.5-4	1,8
GROUND	0,11	20	150	0,19	0,25	1.5-3	
POLISHED	0.05	50	250	0.19	0,24	4,0-6	2,5

Boundary film: ASB stearic acid

II.4.3. Conclusions

These results will be discussed in section III. These tests lead one to the following conclusions:

- The WA and W_α loads vary in the same direction as the mean curvature radius β of the heights of asperities of the surface. Figure 2.4. shows the development of $WA = f(\beta)$.

- When the slip tests are carried out on sample A, the friction coefficient is high throughout the experiment (μ smooth before WA = 0.3, μ mean after WA = 0.3). The WA load was very low during this test, and the protection role of the boundary layer is limited in this particular type of contact. Like very low loads, before WA which characterizes the end of the lubricating efficiency, the beneficial lubricating role of the boundary film must be moderated which would explain the elevated value of the friction coefficient.

II.5. Role of Hardness /23

11.5.1. Experimental conditions

The friction pieces are the same as those used previously (curvature radius 6 mm polished, in a cobalt base alloy). Two plates of different hardnesses were tested:

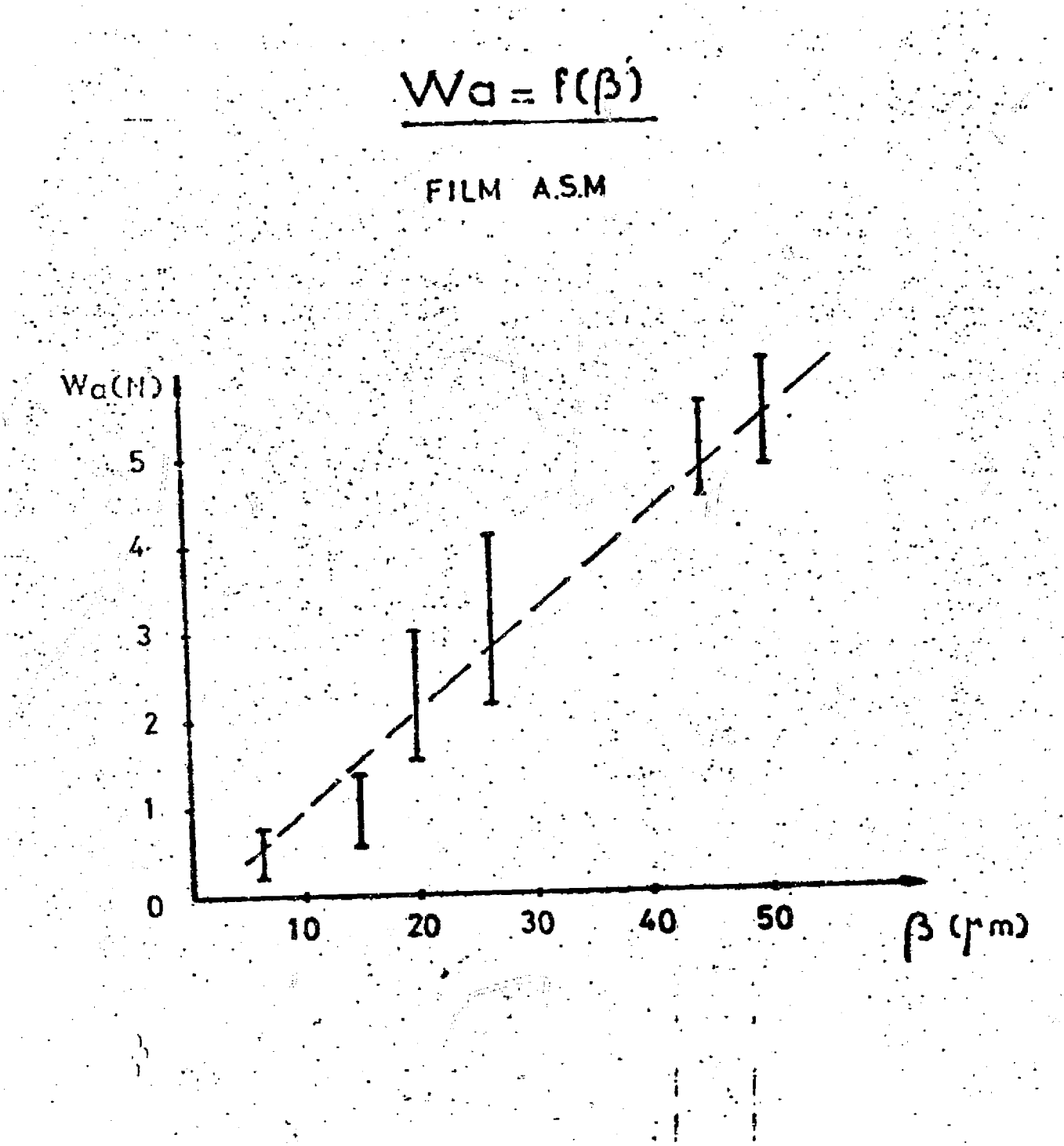

FIGURE 2.4

- A cobalt block with hardness Hv = 400
- A cobalt base alloy of hardness Hv = 610

These plates are diamond polished (roughness RMS 0.05 µm). The tests could be carried out while the plates were immersed in the stearic acid -- cyclohexane (ASB) solution, the boundary film then being equivalent to a monolayer of stearic acid.

II.5.2. Results

The table below shows the loads WA and Wα obtained during tests with and without slip. The results indicate the mean values of loads obtained on many test pieces.

MATERIAL	Cobalt	Co BASE ALLOY
HARDNESS-Hv	400	610
Wa (N)	3.5	5
Wα (N)	1,5	2,5

II.5.3. Conclusions

- WA, a load characteristic of film rupture in slip varies in the same direction as Wα, whose load shows "static penetration" of the boundary lubricated contact,

- These loads increase when the hardness of the metal increases.

- Some objections can be made to the results because the two materials have different chemical compositions. However, in the two cases, the control of the quantity of adsorbed polar molecules has shown that the film obtained was equivalent to one monolayer assumed to be uniformly divided.

- These tests could be made on plates obtained by tempering steel 100 C6 at different temperatures (the results are shown in Appendix C). The WA load varies as well in the same direction of hardness.

- During experiments on contact resistance, it has been shown [16] that rupture of an insulating film results in loads which are lower than the hardness of the substrata was low.

The hardness parameter always depended on the composition of the body (the chemical elements or the metallurgical phases) and it is theoretically difficult to obtain strictly identical films on the surfaces. Cross checking of various experiments tends to show that hardness is a tested parameter during these tests.

II.6. The Role of the Macrogeometry of the Contact

II.6.1. Experimental Conditions

Some experiments on slip were carried out with hemispheric friction pieces of different curvatures. These friction pieces are ball bearings of various diameters and the plates are diamond polished cobalt blocks. In order to correctly visualize part of the electrical contact resistance in our range of measurement, another part of the boundary lubrication process has been recognized by others [17] and called "mass", and the boundary film used was a film of varnish diluted in acetone. In effect, this mass, a quantity of the boundary film, was removed by the friction piece during tangential motion and is slightly visible during other tests given the slight distance covered by the friction piece on the plate. /24

II.6.2. Results and Conclusions

Figure 2.5. shows the aspects of recording electrical contact resistance and the aspects of contact at 50 N for four friction pieces with diameters 2, 3, 4, 8 mm.

- The transition WA load, in the case of contact, does not appear in the field of loads studied except for friction pieces with small curvature radii.

- The "electrical" behavior of the contact is very much related to localization between the friction piece and the plate of this so-called mass [17], and the deformation in geometry of the interface.

This contact deformation is conveyed by the depth of the groove left on the plate during friction, the plastic outflow the length of the groove, and the presence of a frontal ridge before the hemispheric friction piece.

ø Ball Bearing mm	Rc = f(W)	localization at 50N of the mass on the friction piece	groove left on the plate at 50 N
2	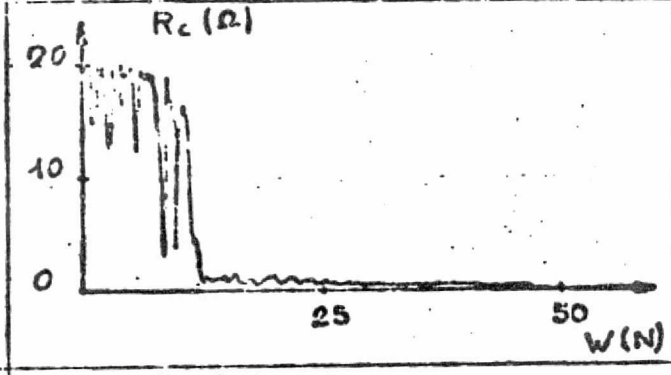	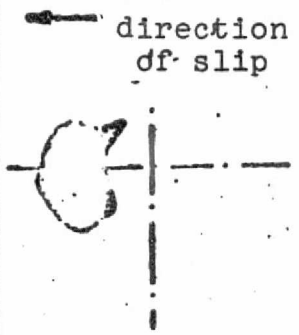	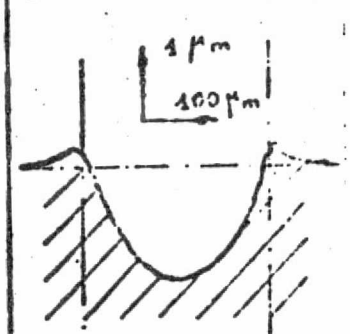
3	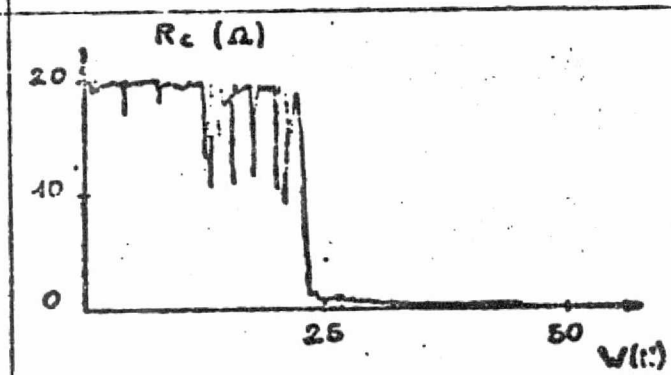	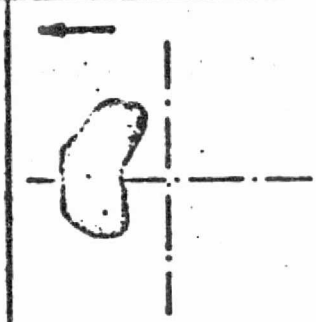	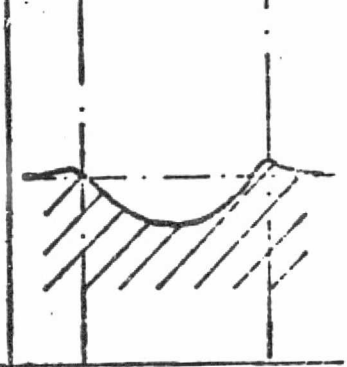
4	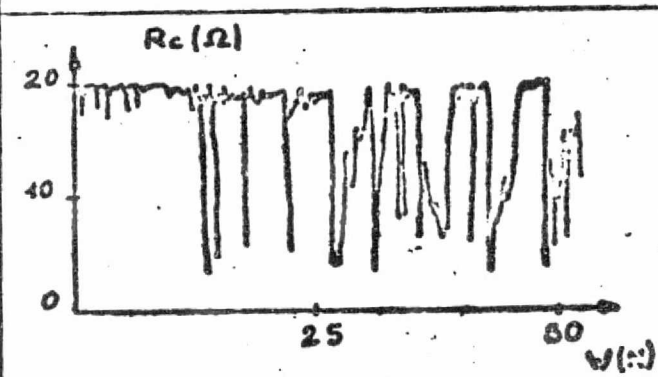	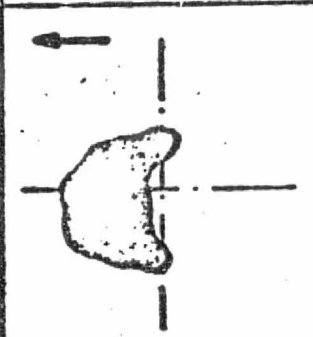	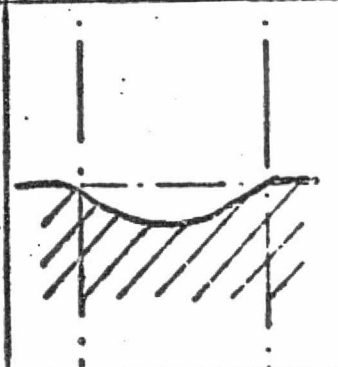
8	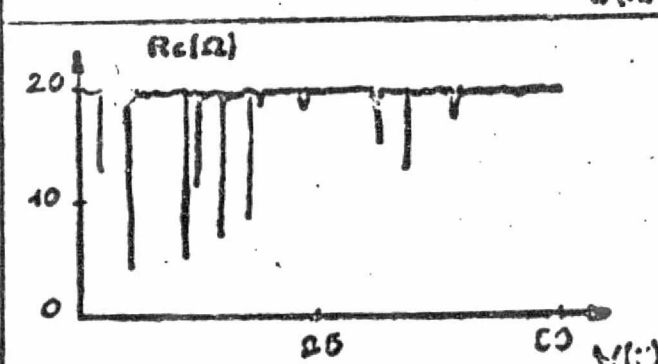	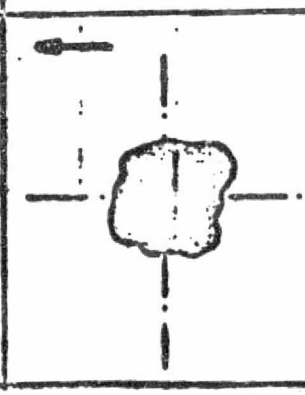	

FIGURE 2.5

PART 3

DISCUSSION

III.1 Application of the Study of Surface Conditions

III.1.1. Analysis of the Roughnesses Used

The real time method of analysis of the surface profiles obtained by a roughness meter (Appendix A) allows us to determine the parameters which characterize the surface conditions of our samples.

- The parameter defining the surface in the Greenwood and Williamson [1] model.

σ : Typical variation of the distribution of height of asperity peaks
β : Mean curvature radius of the peaks of asperities
N : Number of asperities per unit of surface

- The parameters defining the surface in the Whitehouse and Archard model [2]

σ^*: Typical variation of the distribution of profile heights
ℓ : length of the correlation, meaning the measurement of the length of the mean wave of surface defects.

Whitehouse and Archard shown that β is proportional to $\frac{\ell^2}{\sigma^*}$, that N is proportional to $\frac{1}{\ell^2}$, that σ is proportional to σ^*. Also, the three parameters, σ, β, N of the Greenwood and Williamson model are not independent but are related according to the relationship

$$N \cdot \sigma \cdot \beta = k \cdot \frac{1}{\ell^2} \cdot \sigma^* \cdot \frac{\ell^2}{\sigma^*} \qquad N \cdot \sigma \cdot \beta = Cte$$

We have tried to verify these suppositions experimentally.

Various parameters and coefficients of proportionality for different roughnesses used in boundary friction are recorded in the following table.

SAMPLE	$\sigma(\mu m)$	$\beta(\mu m)$	N/mm^2	$\sigma^*(\mu m)$	$l(\mu m)$	β/l^2	N/l^2	σ/σ^*	$\sigma.\beta.N$
A	5,79	6	50	6,3	25,3	0,049	0,032	0,92	0,0015
B	2,05	44	15	2,23	43,6	0,043	0,033	0,89	0,0014
C	0,76	15	95	0,80	16,5	0,049	0,026	0,85	0,0011
D	0,44	26	100	0,51	14,8	0,053	0,025	0,87	0,0012
GROUND	0,11	20	150	0,13	7,3	0,049	0,008	0,85	0,0003
POLISHED	0,05	50	200	0,06				0,84	0,0005

[Commas in the tabulated material are equivalent to decimals.]

The theoretical proposals of Whitehouse and Archard resulting from the relationship of σ, β, N = Cte are verified in cases of surfaces obtained by different microball tests (A,B, C,D). For these four surface conditions, $\sigma \cdot \beta \cdot N = 0.0013$ (mean value). For the polished or ground samples, the product $\sigma \cdot \beta \cdot N$ is different and equal respectively to:

$$\sigma \cdot \beta \cdot N = 0.0003 \text{ for the ground surface}$$
$$\sigma \cdot \beta \cdot N = 0.0005 \text{ for the polished surface}$$

The dependence of the parameters σ, β, N which has been shown using theoretical models has now been verified experimentally /27 in the case of ground surfaces ($\sigma \cdot \beta \cdot N = 0.0013$). In effect, the sandings make it possible to obtain surface conditions with an aleatoric aspect, without texture which verifies the hypotheses of ergodicity of theoretical models and which can be defined from analysis of a profilometric summary in two dimensions. The application of these models is perhaps misused for polished or ground surfaces, these surfaces showing a texture which can be explained by the product $\sigma \cdot \beta \cdot N$ being different. In spite of everything, we have used these models for simplifying the reasoning.

III.1.2. Study of Contacts

Smooth Ball -- Plane of Roughnesses Used

These different plates in which the analysis of roughness figures above can be produced during friction by a polished hemispheric friction piece with curvature radius 6 mm. The contact model developed by Greenwood and Tripp [13] (Appendix A) can be applied to smooth ball-rough plane contacts.

It is apparent, that at the level of WA loads, where evolutions in the boundary lubrication contact are produced, the number of asperities in contact were small (2 to 3 asperities per contact). The profilometric summary of the plates and the end of the friction piece (at the same vertical amplification) makes it possible to visualize this result (figure 3.1).

An example of the results furnished by the Greenwood and Tripp model compared to that of Hertz (for a smooth plate). This is illustrated below:

HERTZ

- radius of a polished and smooth friction piece 6 mm
- ideally smooth plate

$$E' = 12200 \text{ Kg/mm}^2$$

$$\frac{1}{E'} = \frac{1-\nu_1^2}{E_1} + \frac{1-\nu_2^2}{E_2}$$

let us assume W = 50 N
- radius of the contact circle = 0.12 mm
- contact area: $4.5\ 10^{-2}$mm
- compliance: $2.3 \cdot 10^{-3}$ mm

GREENWOOD AND TRIPP

- friction piece radius 6 mm
- plate $\sigma = 0.76$ m
  $\beta = 15$ µm
  $N = 95$ /mm^2
- in the case of Wa obtained: from 0.4 to 1.2N (stearic acid film) let us assume W = 50N
- effective radius of contact: 0.17 mm
- actual contact area: $1.4 \cdot 10^{-2}$ mm
- number of asperities in contact: 8 at a load of 50N, slightly higer at Wa, the number of asperities in contact is limited
- compliance: $1.6 \cdot 10^{-3}$ mm = 1.6 µm

This small number of asperities in contact is plasticized. The loads corresponding to the onset of plasticization are very low for the asperities of the surfaces studied:

SAMPLE	A	B	C	D	GROUND
Plasticization load of one asperity (N)	$0.06 \cdot 10^{-3}$	$3 \cdot 10^{-3}$	$0.36 \cdot 10^{-3}$	$1.1 \cdot 10^{-3}$	$0.65 \cdot 10^{-3}$
Wa (N)	0.2 - 0.9	4.5 - 5.3	0.4 - 1.2	2.5 - 4	1.5 - 3
Contact asperities	2 to 3	2 to 3	2 to 3	2 to 3	2 to 3

SAMPLE

B

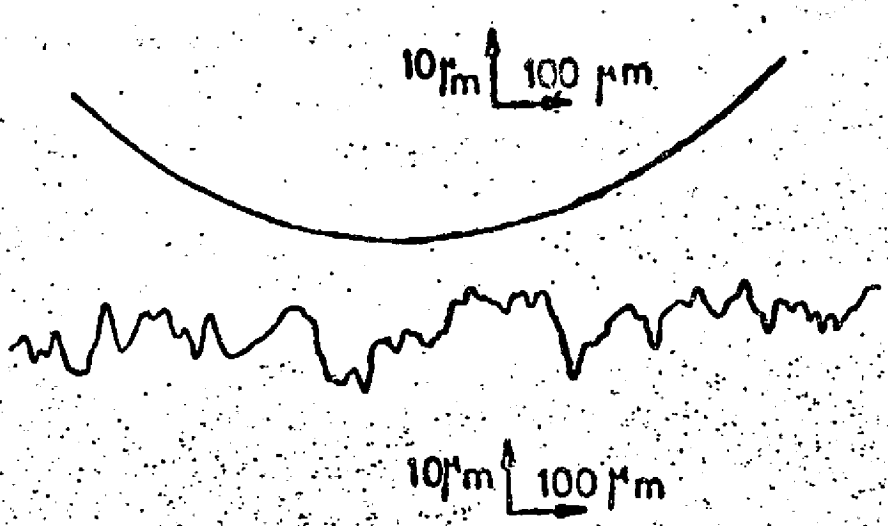

SAMPLE

D

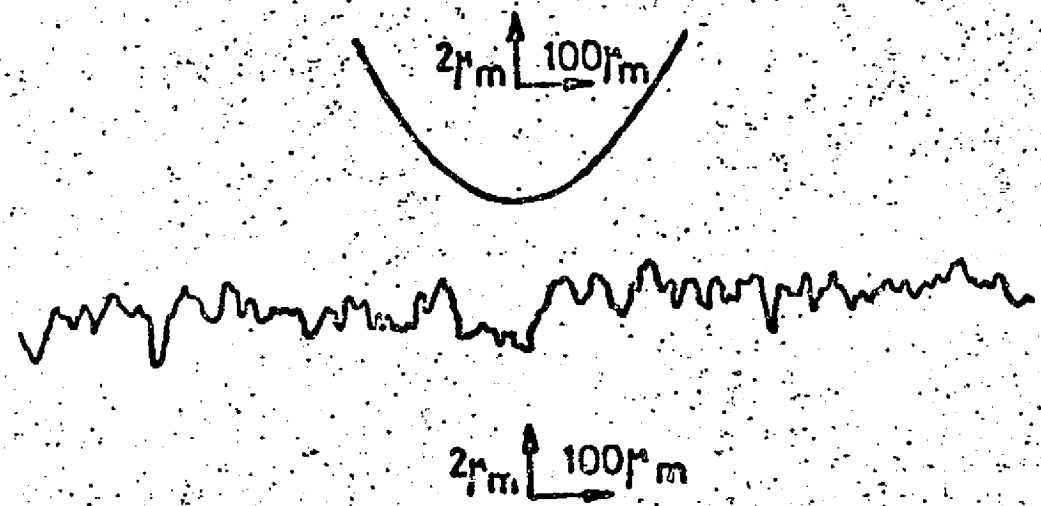

Profilometric record of the plates and

the end of the friction piece

FIGURE 3.1

The asperities were plasticized, and their curves are deformed. However, the calculation of Greenwood and Tripp based on the hypotheses of elastic deformation is valuable for studying the number of contact asperities. In effect, in the field of load studied deformation of the substratum is elastic and plastic deformation is limited to the peak of asperities and is not of interest except as a small part of their height. Greenwood [18] points out that the plastic displacements at the asperity level are limited to a slightly different amplitude than that of elastic displacements, the excess of load contributing to total deformation of the substratum (elastic in the case of the Greenwood and Tripp model). /29

It has been proved as well that during plastic macroscopic contact, plastic deformations of the asperities are limited: the roughness of a surface persists at the base of the hardness impression [19].

A precise study of roughnesses and contact used results in the following elements:

- the number of contact asperities n is small: 2, 3 at Wa
- the asperities are deformed plastically, but this plastic deformation is limited to the peak of the asperities, and is of interest only in the low part of their height.
- the parameters σ, β, N of roughness are not independent.

III.1.3. Recurrence at Wa Characteristic Load of the Rupture of the Boundary Layer

We have succeeded in showing experimentally that WA is related to the curvature radius of the asperity peaks. It has been suggested [20] that the peaks of the asperities are parts of the surface resulting during friction, without this having been proved experimentally.

Although the number n of contact asperities was constant (2 or 3) and only their higher parts were involved in the contact, Wa is not independent of N, the number of asperities/mm^2 and the σ variation of type of distribution of the peaks of the asperities, because the three variables σ, β, N are related according to the relationship σ. β. N are related according to the relationship $\sigma \cdot \beta \cdot N$ = Cte, as has been shown experimentally in the preceding pages.

Scruton and Tabor [21] have shown that in the elastic contact condition (glass friction piece on glass plate), the slip force of the boundary film was related to actual contact pressure. Friction pieces with different curvature radii were used. The Hertz model shows that actual contact pressure

is related to the curvature radius of friction piece R:

$$W = \frac{4}{3} E' R^{1/2} \alpha^{3/2} \qquad A = \pi R \alpha$$

from which $A = \pi \left(\frac{3RW}{4E'} \right)^{2/3}$

Contact pressure : $p = \frac{W}{A}$

$$p = \frac{1}{\pi} \left(\frac{4E'}{3} \right)^{2/3} \frac{W^{1/3}}{R^{2/3}}$$

But the idea of burning the boundary film due to actual contact pressure cannot be used to explain the variations of WA with β, because, the asperities were plasticized, the actual contact pressure at the level of asperity is constant and equal to the plastic outflow pressure of the material: p = 0.4 H, H being hardness.

The analysis of results furnished by contact resistance will suggest an interpretation of rupture of the boundary layer during friction.

III.1.4. A Balance Sheet of the Study of Contact Surfaces/30

- β radius of curvature of the peaks of asperities is the parameter of roughness affecting WA, the characteristic rupture load of a deposited boundary film.

- The development of $W_A = f(\beta)$ varies according to the boundary film deposited. Two tests in Section I were carried out with two roughnesses of different plates giving the aspect of development Wa = f(β) for a cyclohexane film.

- The results are summarized in Figure 3.2.

III.2. Contribution of the Analysis of Contact Electrical Resistance

III.2.1. Static Test Compared to Dynamic Test

- Dynamically, between zero load (beginning of the test) and Wa, the value of resistance varies with a large amplitude and frequency. The main value is several ohms and decreases when the load increases from zero to Wa. Above Wa, the value of resistance changes slightly: The mean value

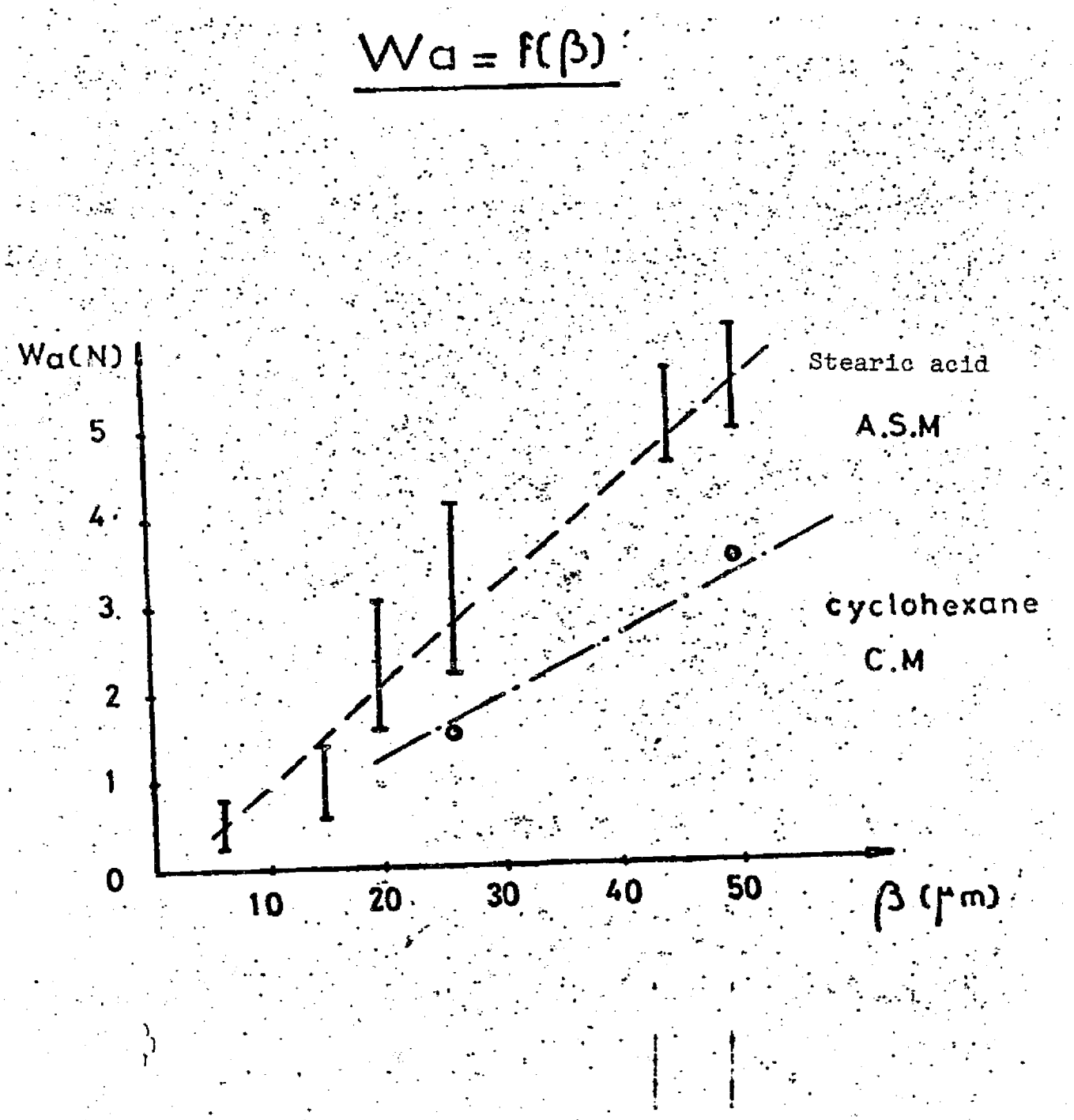

FIGURE 3.2

is very low and decreases toward zero as the load increases. If, at a given load W' lower than Wa, one makes a test on friction, the oscillations of contact resistance occur around a given mean value which is constant (figure 3.4.). This mean value was equal to the mean value which these oscillations produced when the load increases during the test, the load passing the value W'.

- Statically, the decrease in resistance is smooth, without oscillations. As has already been pointed out, at a given load, the value of contact resistance statically is higher than the value of mean dynamic resistance and at a given W" this value of static Rc is constant without evolution even with time of application of the load.

The figures (3.3, 3.4) and the table below show a comparison between static and dynamic tests. The boundary film is stearic acid (ASB), the plate is rough (σ = 0.42 µm β = 26 µm)

	W(N)	0.1	0.3	0,7	1	1,5	2,5	5	10
DYNAMIC	MEAN Rc TEST AT W (Ω)	17	10	4	2	1	0,5	0	0
DYNAMIC	MEAN Rc TEST AT W = cte (Ω)	17	10	4	2	1	0,5	0	0
STATIC	Rc (Ω)	>20	>20	>20	≈20	17	13	5,5	2

Conclusions /34

- The insulating properties of the boundary layer are weakened by tangential motion.

- As to static or dynamic tests, the rate of load increase does not affect the values of contact resistance.

Dynamic: Mean Rc at W' = cte is equal to the mean value obtained during the test with increasing load when the load passes the value W' (several ohms if W' < WA, zero if W' > W_A).

Static: The resistance of contact W" = cte does not evolve as a function of time.

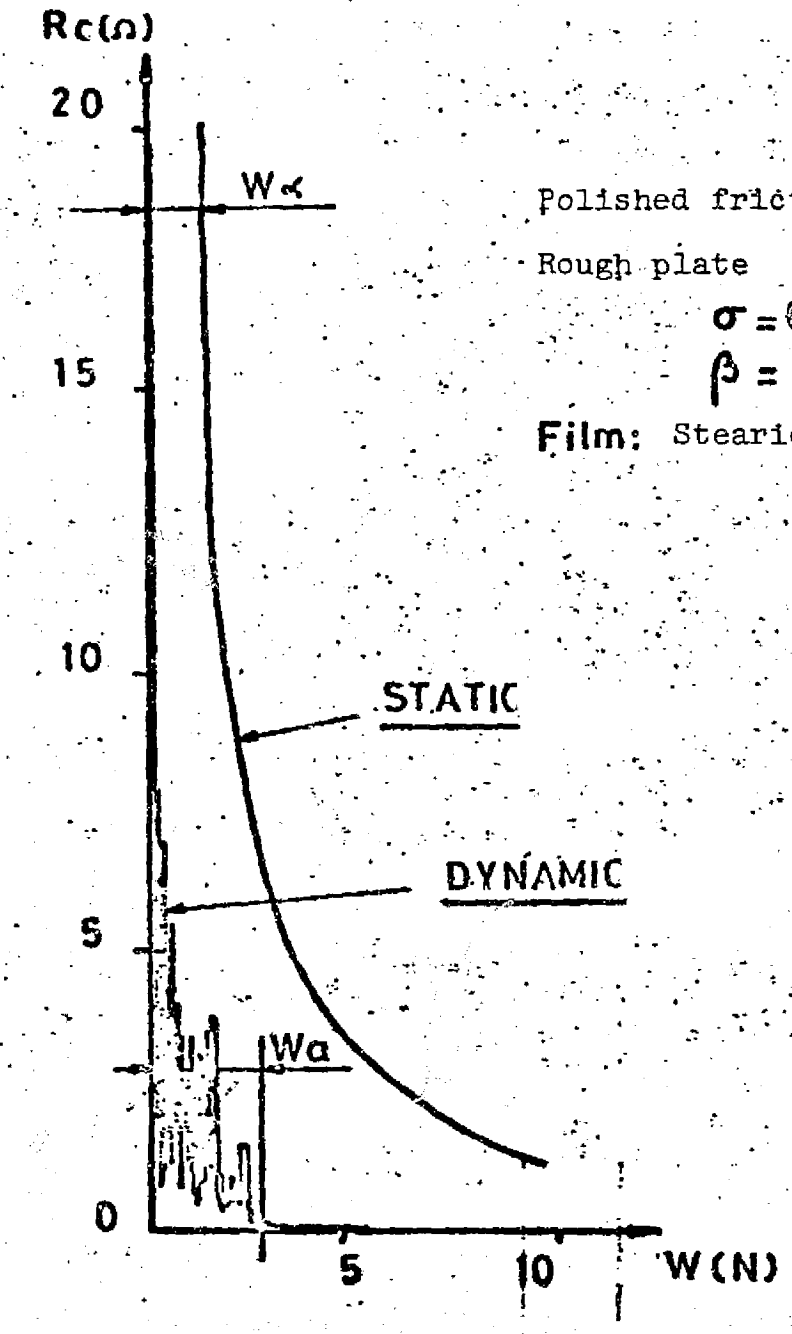
Rc(Ω)
20
15
10
5
0
Wα
Wa
STATIC
DYNAMIC
5
10
W(N)
Polished friction piece
Rough plate
σ = 0,42 μm
β = 26 μm
Film: Stearic acid

FIGURE 3.3

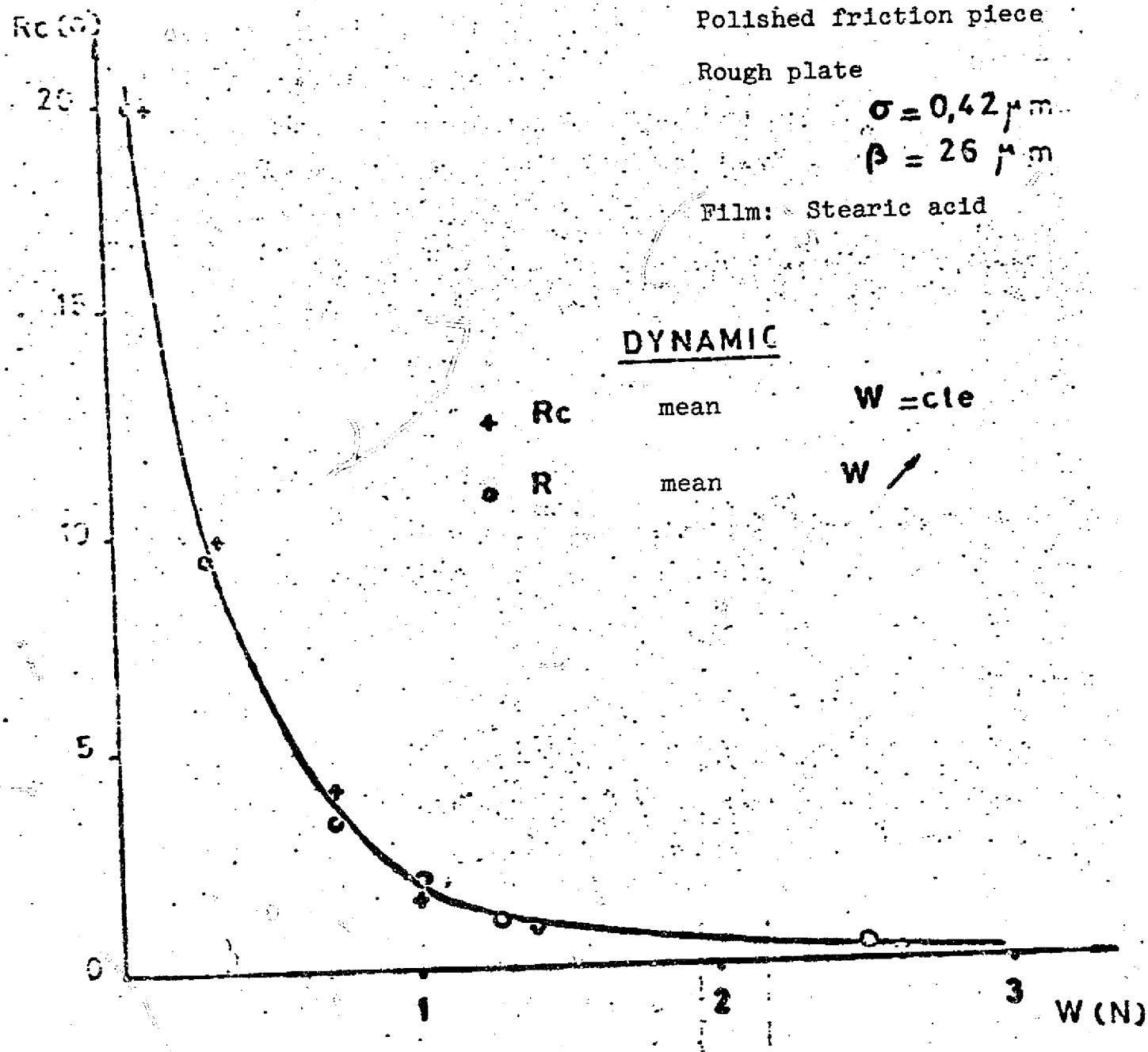

FIGURE 34

This can be explained by the fact that during the test at an increasing load, the rate of increase of the load is very low. This parameter can interferewith the validity of experiments.

III.2.2. Study of the Decrease of Static Rc = f(W)

The decrease of static Rc = f(W) follows the power law in the measurement field (0.20Ω): $Rc = \frac{k}{W^n}$. The theoretical laws of actual contact and ideal polishing give n = 1/3 or n = 1/2 according to whether this contact is elastic or plastic [22]. But, the exponent n obtained during the test must always be higher $1.5 < n < 2$. For the preceding static test cited, during comparison of static and dynamic testing (figure 3.3) n = 1.5. The following interpretation has been proposed to explain these elevated exponents: when the load increases, the surface is rough, the number of asperities in contact increases. A statistical model has been developed to this effect [16]. However, in the field of load testing (0, 10 N), the number of asperities in contact remains low (2 to 3). This shows that the elevated exponents of the laws of decrease are not due to an increase in the number of asperities in contact or to an increase in plastic deformation of these asperities. The interpretation will truly be related to the phenomenon of penetration of the adsorbed insulating boundary layer, a process related to deformation of the substratum during this penetration.
Therefore, the boundary lubricating film will be considered as an entity composed of adsorbed polar molecules, surface impurities, oxides and the first layers of the metallic substratum subject to deformation. The static penetration of a thin film has been studied experimentally in a very particular case.

III.2.3. A Particular Experimental Model of Penetration of a Thin Film.

Knowledge of deformation of the entity of the composite surface previously defined seems necessary to the study of maintaining a boundary lubrication film. For simplification, we have studied a particular depression of a homogeneous thin film, purely plastic, in an experimental model (the superficial lubrication boundary films have a solid structure being composed of adsorbed molecules on a substratum of solid metal and oxide).

III.2.3.1. Experimental Arrangement /35

A thin film of paste for modeling is deposited on a glass sheet. We will study the penetration of this layer with increasing load (the rate of increase of the load being very low) by a glass cupel. The cupel simulates an asperity on the surface and the layer of paste on the model simulates the boundary film. As a function of the load, we will experimentally

determine the thickness of the paste for model h which remains in contact as well as surface S of the cupel in contact with the layer of modeling paste. We will suppose that electrical resistance of such an interface is in the form $Rc = \frac{kh}{S}$ and we will be interested in the evolution of the relationship of $\frac{h}{S}$ with the load.

Two series of tests were carried out:
- thickness of the paste 50 µm
  cupel Ø 147 mm
  cupel Ø 248 mm
  static depression from 0 to 75 N.
- thickness of the paste 140 µm
  cupel Ø 147 mm
  static depression from 0 to 75 N.

III.2.3.2. Results

Thickness of the paste is 50 µm, cupel Ø 147 mm

Figures 3.5, 3.6 show evolution of S, h, $\frac{h}{S}$ as a function of load.

- Going from a certain load (50 N), one cannot penetrate further into the layer of modeling paste: it remains at a boundary thickness h in the contact of approximately 25 µm of thickness.

- Beyond this load, the surface S continues to increase, this increase being due to elastic contact deformation.

- The law of decrease of resistance of Rc contact modeled according to the relationship $\frac{h}{S}$ follows a power law $Rc = \frac{k}{W^n}$. As long as one does not reach a maximum thickness, the exponent n is large (n = 1.12). On the other hand, once the boundary thickness is reached (the variations of $\frac{h}{S}$ then being uniquely caused by deformation of the body in contact), the exponent n is smaller (n = 0.33): one proves the exponent 1/3 given by theoretical studies of contact resistance.

- Thickness of the paste 50 µm, cupel 248 mm

One obtains the same boundary thickness, but it is obtained for a higher load (63 N) figure 3.7.

- Thickness of the paste 140 µm, cupel Ø 147 mm

The boundary thickness is not reached in the load field and the contact resistance assumed in the form $\frac{h}{S}$ follows a power law $Rc = \frac{k}{W^n}$, n being constant and equal to 1.12 in the field of loads tested.

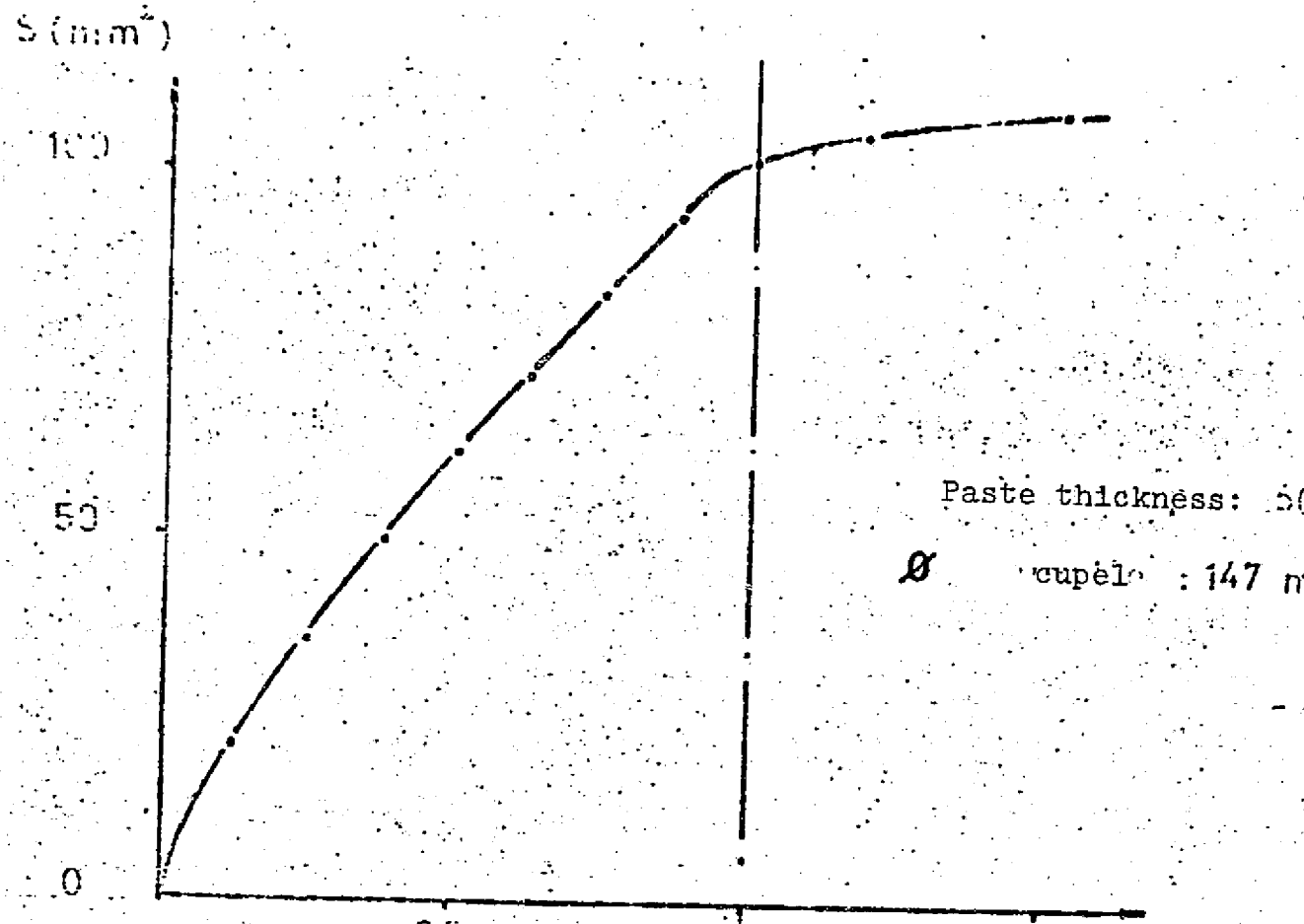

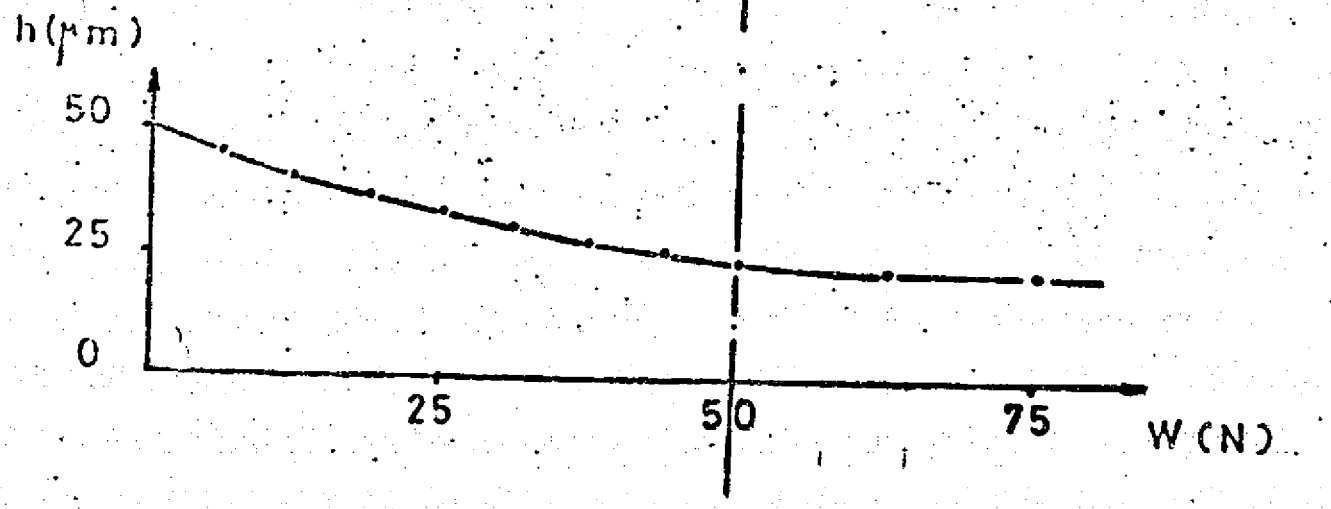

FIGURE 3.5

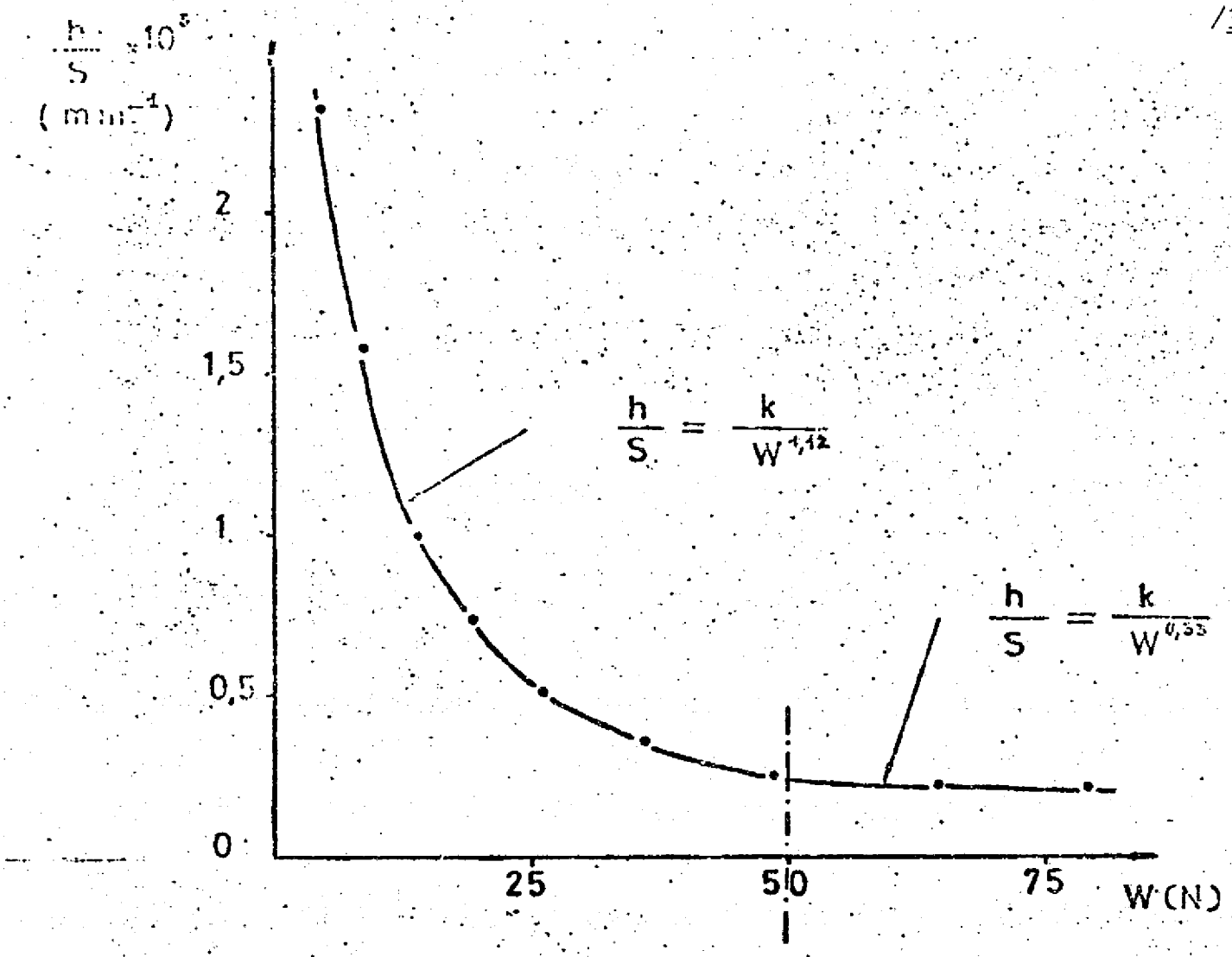

. Paste thickness : 50 µ m

Ø cupel : 147 mm

FIGURE 3.6

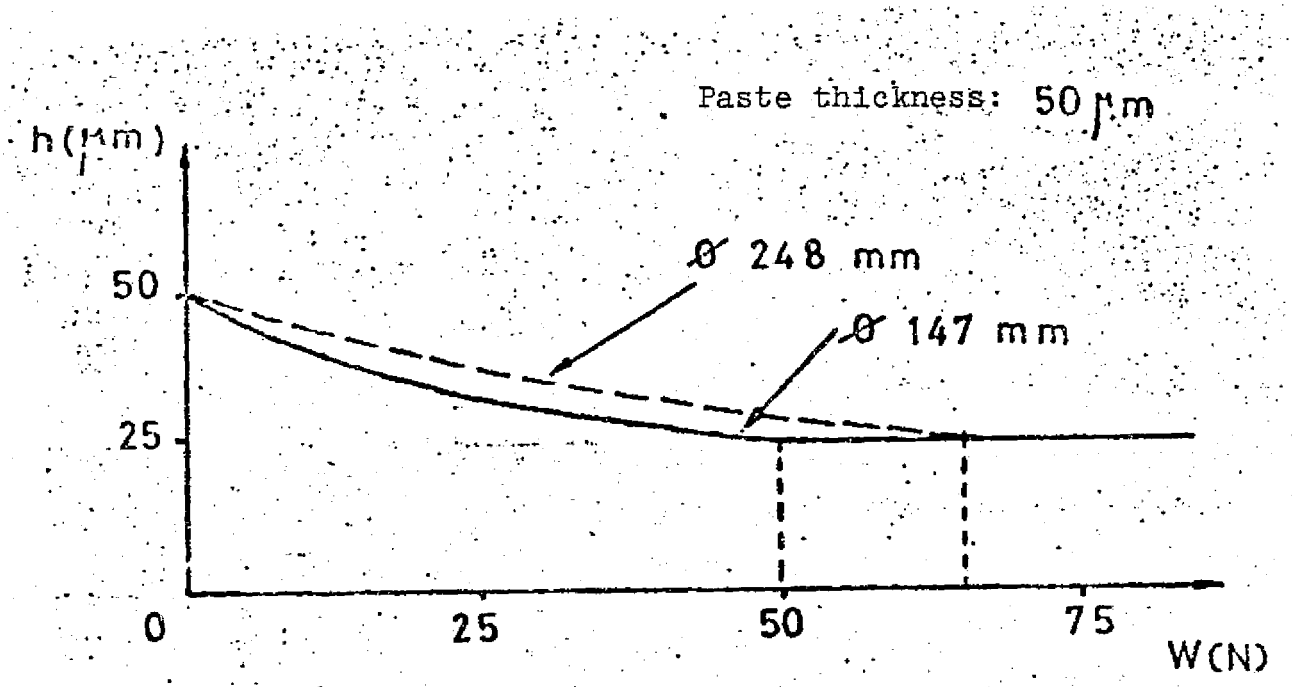

FIGURE 3.7

III.2.3.3. Conclusions

One evidently cannot draw general conclusions of this very particular experimental model. However, in this case, during static penetration, we note:

- A boundary thickness, boundary h can be reached.

- The exponent of the curve of decrease is elevated (1.12) since it penetrates the deposited thin film, being 0.33, given for theoretical models of elastic contact, once the thickness reaches the maximum.

III.2.4. Balance Sheet of the Analysis of Variations of Contact Resistance with Load. /39

- The insulating property of the boundary film is weakened by tangential motion. The film can support elevated loads statically and be broken by weaker charges during slip. The dynamic test compared to the static test shows that, from the point of view of contact resistance, it behaves causes a decrease in height of the boundary film in relation to the height which this film would have with the same load in a static test without slip.

- The coefficients of elevated n of decreasing curves Rc = f(W) are due to penetration of the boundary entity previously defined; this can be verified in a particular experimental model of a plastic thin film.

- The rupture of the boundary film produces loads which are more elevated in static tests than in dynamic tests provided that the contact of the friction pieces on the asperities (numbering two or three) has already reached the stage of plastic deformation. This makes one think that in static, it occurs in a field of elevated loads at a certain boundary thickness of the lubricating layer very difficult to discriminate from contact. The particular experimental model of penetration of a thin plastic film shows clearly that a maximum critical thickness h has been reached.

These conclusions make it possible to produce a mechanical model of rupture of the boundary lubrication film developed in the next paragraph.

III.2.5. The Model Suggested by the Preceding Statments.

III.2.5.1. The Aspect of Deformation of the Boundary Film:

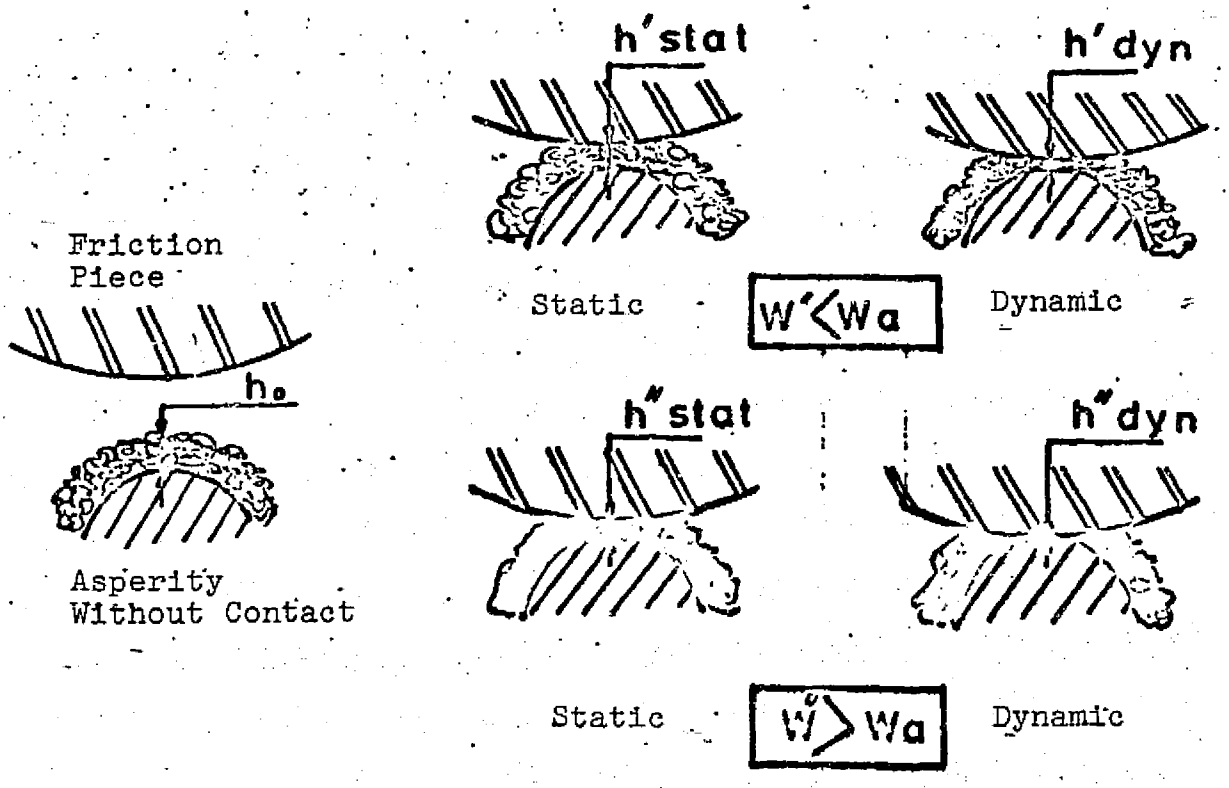

- When $W' < W_A$, in static, it produces penetration of the boundary film, penetration increases due to tangential motion dynamically (the results are suggested by the values of contact resistance). /40

$$h_o > h' \text{ stat} > h' \text{ dyn}$$

- When $W'' > W_A$, the static penetration of the film is larger than that obtained with the static load W', the rupture not always being reached necessarily at this load W".

$$h'' \text{ stat} < h' \text{ stat}$$

The contact is deformed plastically and this thickness h" seems to tend toward a critical thickness h" which is difficult to discriminate from contact.

Dynamically, this critical thickness cannot be diminished and the film will be cut and broken:

$$h'' \text{ dyn} = 0$$

Also, during slip, the rupture of the lubricating boundary entity does not occur if this critical thickness h" is attained.

III.2.5.2. Parameters Affecting this Critical Thickness

- This critical thickness evidently will be affected by the chemical aspects of the adsorbed boundary film (length lo of the adsorbed polar molecule, for example).

- The smaller the radii of curvature of asperities β become, the easier critical thickness ho will be reached; this is visualized by testing depression of the paste layer in the model by cupels of different diameters. The asperities will be plasticized and deformed without the film being broken (the actual contact pressure will then be equal to the pressure of the outflow of the material). Then, the curvature of the asperities will indirectly affect the rupture load W_A of the film, its role being to permit attaining the critical thickness hc defined during static testing, more or less rapidly according to the load applied.

- Facility of contact deformation affects critical h equally. In effect, during tangential motion, the contact deformation is increased (swelling, increase in the contact area). These points will be discussed in the following section. This increase in plastic deformation of the interface causes an increase in the surface protection by the boundary film in the contact. The quantity of boundary film held in the contact must then be "spread out" more in order to ensure lubrication and critical thickness hc is then reached more easily and contact deformation is large. This is shown by tests carried out, on the one hand, with plates of different hardness and on the other hand with friction pieces of different curvatures.

- The problem of the mass: encountered in a number of tests of boundary lubrication, this mass is comprised of the debris of the lubrication layer caused by the hemispheric friction piece during tangential motion. The tests have shown (figure 2.5) that according to the geometry and contact deformation, this mass could enter into the friction piece and plate interface. Also, in certain contact conditions, the friction /41 occurs by intervention of this mass which "feeds" the lubrication film of the interface giving a thickness which is always higher than the critical h.

III.2.5.3. Balance Sheet of this Model

- The rupture of the film is related to critical thickness hc at its connection to the substratum, τ

$$Wa = f(hc, \tau)$$

- hc is a function of:

  - the nature of the film ξ
  - curvature radius of asperities β.
  - contact deformation.
    microscopic: related to β and to hardness H
    macroscopic: related to H and to the curvature of the friction piece C.
  - formation of the mass A related to ξ and C.
    A and ξ represent the chemical nature of the contact.
    β and C are representatives of the contact geometry.
    H is the induced plastic characteristic of the metal

III.3. Contribution of Microscopic Observation of the Samples.

These observations confirm the increase in contact deformation during tangential motion. This increase in deformation amplitude affects the critical thickness hc, as we have seen: the effect of tangential motion causes an increase in the contact area [23], the surface to be protected by the film in the interface is larger, the thickness of the lubrication entity was smaller. But the slip also produces the formation of a plastic frontal protrusion pressed back in front of the friction piece (figure 3.8), as well as the outflows of the material the length of the friction groove. This particular deformation, studied by many authors [24] for contact of a ball bearing and plane is clearly visible on the tests in figure 2.5. As has been pointed out, it produces a back flow of smooth type from this swelling or tearing of the frontal protrusion if the deformation becomes too important. One can also well imagine, and the tests show it (figure 2.5), that the breadth of the swelling was dependent on the load applied, the hardness of the plates, the curvature of the friction pieces and the parameters will affect the "plowing" of the frontal protrusion by the hemispheric friction piece and, from this the rupture of the boundary lubrication film visualized in our method of operation by abrupt decrease in contact electrical resistance. This process will cause deformations of a "severe" type defined in Section I and can explain the transition in the contact deformation aspect during a pass at low W_A:

- deformation of the "fresh" type (scratches of plastic type before W_A).
- deformation of "severe" type (lifting after W_A).

This evolution in the method of degradation as a function of load is clearly visualized by Kragelsky's experiment [25], carried out with a particular contact model (Appendix B).

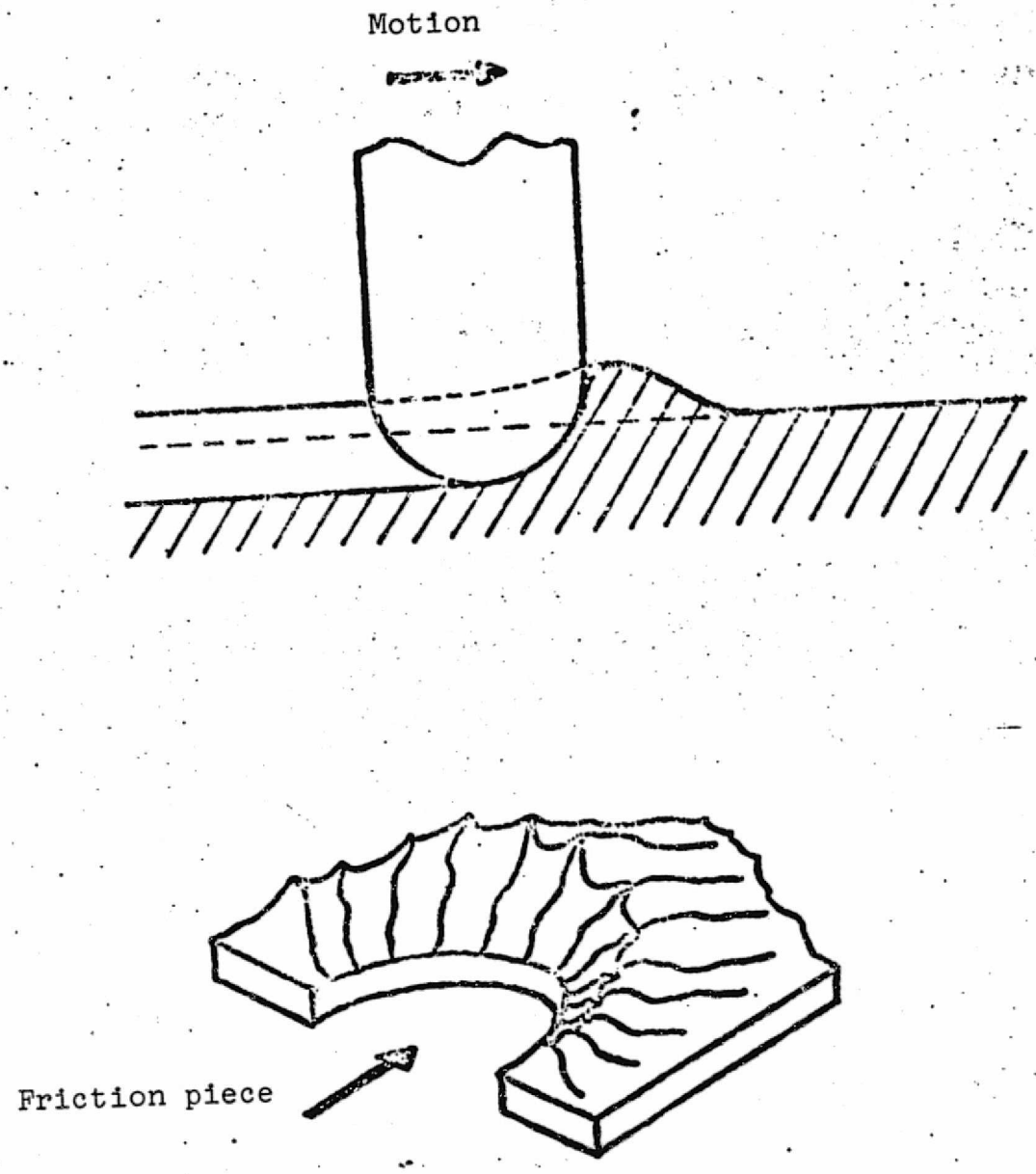

FIGURE 3.8

- These plastic deformations (increase in contact area and formation of swellings during slip) cause dislocations and bands of slip. The increase in amplitude of deformation and tangential motion have then the effect of creating the maximum emergence of slip bands and increase the percentage of "new" surface then for protecting the boundary lubrication film caught in the contact. /43

This part of the lubrication film caught in the frontal zone between the hemispheric friction piece and part of the swelling which is in contact are subject to large constraints. The critical thickness hc is reached more easily because the breadth of the swelling increases with load. This frontal protrustion affecting critical thickness hc will be a process which also conditions the rupture of the boundary lubrication film.

CONCLUSION

- The transition load W_A is very important because it is characteristic of the evolution of wear and deterioration of the mechanical elements evoked in the boundary lubrication process.

- We have developed a particular experimental methodology in studying the boundary lubrication film by the type of manipulations used. In this particular type of contact, we have attempted to classify the parameters which, in practical industrial reality, can affect the boundary lubrication. A pair of mechanical elements will function well as long as deterioration of the surfaces protects the "fresh" aspects (aspect defined before W_A for all experimental methodology), one such procedure being dependent on:

  - adsorbed boundary film.
  - contact microgeometry (roughness).
  - macrogeometry.
  - material used (hardness).

- The experimental methodology used has the following original points:

  - The evolution of W_A with curvature radius β of the peaks of asperities furnishes the proof that β is the parameter of roughness affecting boundary lubrication.

  - W_A depends on the chemical character of contact (boundary entity) and on the geometric and mechanical aspects of this contact. Analysis of contact electrical resistance makes it possible for us to suggest a model showing the relationship between the chemical and mechanical processes of boundary lubrication.

  - This experimental methodology makes it possible to foresee studies in more detail before one can present a rheologic characterization of boundary films, in particular, the rheologic-physiochemical relationship of the film.

For the moment, it seems necessary to have a grasp of the parameters and processes studied previously in order to have a good comprehension of the boundary contact in mechanical applications.

APPENDIX A

/45

STATIC CONTACT AND CHARACTERIZATION OF ROUGH SURFACES

No surface used mechanically is perfectly "smooth". All of them show roughness on a more or less microscopic scale. Let us assume two elements whose surfaces are pressed together under a load W. The contact will occur at certain points and the actual contact area Ar will not be more than a part of the apparent contact area Aa (Figure A1).

A microgeometric characterization of the surfaces, as exact as possible, was necessary then for studying static contact between mechanical pieces.

Of the many contact models which have been developed, the most important are those of Greenwood, Williamson and Tripp [1, 13], Whitehouse, Onions and Archard [2, 26]. Besides a precise characterization of rough surfaces, these models study two types of contact: the contact plane rough polished plane, the contact rough plane and smooth ball bearing. We will consider these different approaches:

- Greenwood and Williamson model
- Greenwood and Tripp model
- Whitehouse, Archard and Onions model.

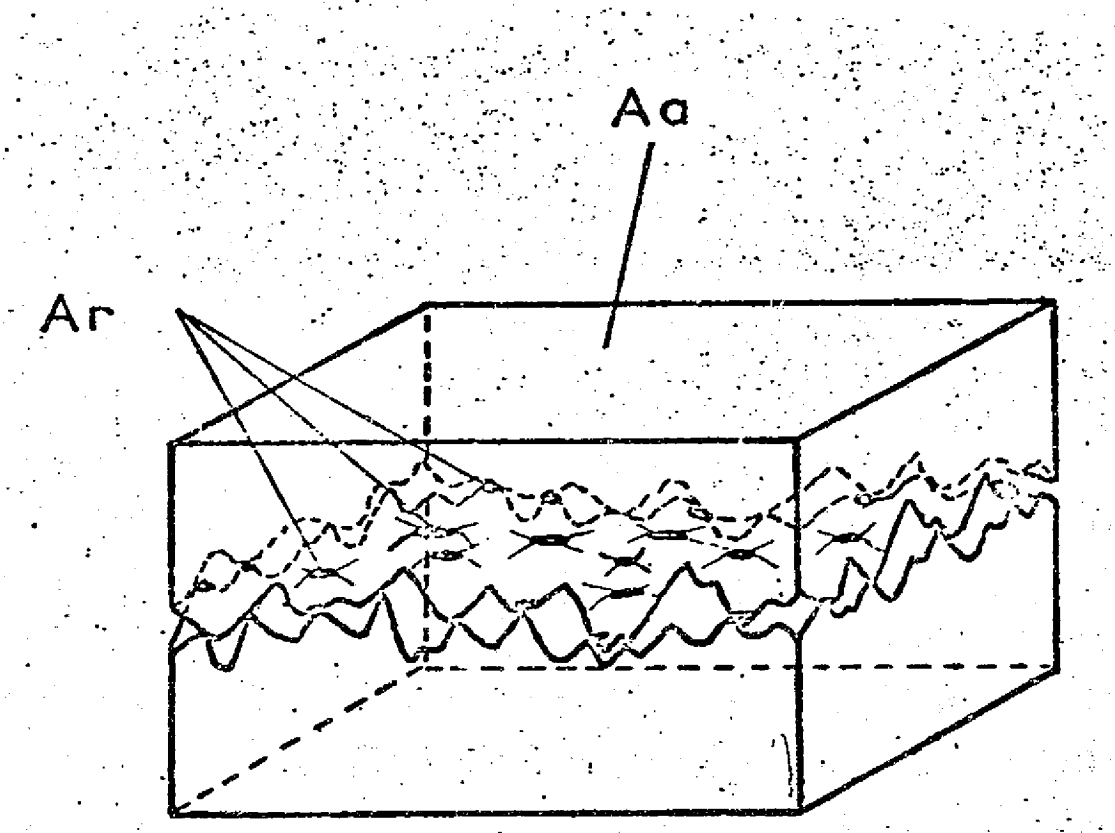

FIGURE A.1

A I: GREENWOOD AND WILLIAMSON MODEL /47

This first study involved contact between a polished plane and a rough surface in which the nominal reference is the plane (fig. A2). The peaks of the asperities are assumed to have the same radius of curvature β. The deformations are considered to be of an elastic type, according to the Hertz theory, for asperity I (figure A3) the contact area Ai, the radius of the circle of contact Ai, the load supported by asperity Pi will be related to compliance α by the following relationships:

$$Ai = \pi\beta\alpha$$
$$ai = \beta^{1/2}\alpha^{1/2} \qquad (1)$$
$$Pi = \frac{4}{3}E'\beta^{1/2}\alpha^{3/2}$$

Let $\Phi(z)\,dz$ be the probability that an asperity peak will be contained between sides z and z + dz. Asperity i will be in contact if the height is higher than U, the distance between the polished plane and the reference of the rough plane. Among the N asperities of the surface, there will then be

$$n\int_u^\infty \Phi(z)\,dz \quad \text{in contact.} \qquad (2)$$

If the contact asperity has height z initially, the compliance at the level of this asperity is then z-u

$$\pi - z = p \qquad (3)$$

If η is the number of asperities per unit of surface, for the /49 apparent contact area a, the relationships (1), (2), (3) make it possible to determine the:

number of contacts: $$N = \eta a \int_u^\infty \Phi(z)\,dz$$

actual contact area $$A = \pi\eta\beta a \int_u^\infty \Phi(z)(z-u)\,dz$$

load supported by the N contacts $$P = \frac{4}{3}E'\beta^{1/2}\eta a \int_u^\infty \Phi(z)(z-u)^{3/2}\,dz$$

In standardizing the variables and supposing $h = \frac{u}{\sigma}$ these relationships become

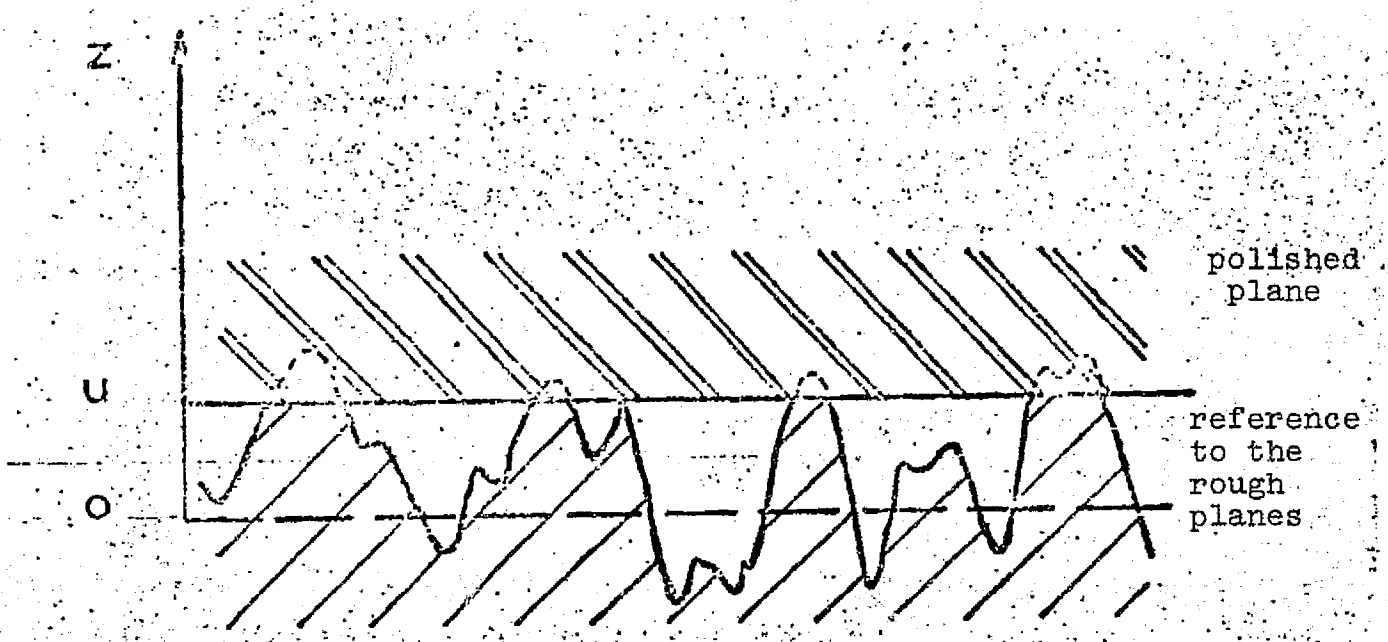

FIGURE A.2

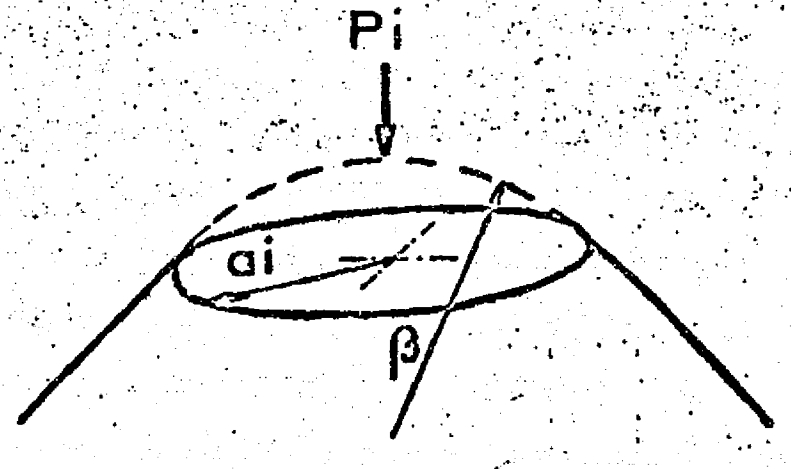

FIGURE A.3

$$N = \eta a F_0(h) \qquad (4)$$

$$A = \eta a n \beta \sigma F_1(h) \qquad (5)$$

$$P = \frac{4}{3} E' \beta^{1/2} \eta a \sigma^{3/2} F_{3/2}(h) \qquad (6)$$

with $$F_n(h) = \int_h^\infty (s-h)^n \Phi^*(s)\, ds$$

The distribution of the heights of asperities are Gaussian for most of the surface profiles.

$$\Phi^*(s) = \frac{1}{\sqrt{2\pi}} e^{-\frac{s^2}{2}}$$

thus $$F_n(h) = \frac{1}{\sqrt{2\pi}} \int_h^\infty (s-h)^n e^{-\frac{s^2}{2}}$$

By resolving the system of equations (4), (5), (6), Greenwood determines the relations connecting the actual contact area A to load P and the real mean pressure of contact $\frac{P}{A}$ at load P. The actual contact area is proportional to the load and independent of the apparent area, the actual mean contact pressure varies slightly with the load.

At the level of the asperity, the plasticization appears /50 at a point of maximum shear for mean pressure mp = 1, 1Y [27], Y being the elastic limit of the metal. These theories of hardness give H = 2, 8Y [27]. Thus, at the beginning of plasticization:

$$mp = 1,1\, Y = \frac{1,1}{2,8} H$$

but $$mp = \frac{P}{\pi a^2} = \frac{4}{3\pi a^2} E' \beta^{1/2} \alpha^{3/2}$$

The critical value of characteristic compliance of the onset of plasticization will verify then the relationship

$$\frac{1.1}{2.8} H = \frac{4}{3\pi a^2} E' \beta^{1/2} \alpha_p^{3/2}$$

$$\alpha_p = 0,89 \beta \left(\frac{H}{E'} \right)^2$$

The plasticized asperities will be such that $z > u + \alpha_p$. Supposing that the "plastic" displacements have an equivalent amplitude to "elastic" displacements, Greenwood uses the model of elastic deformation for studying the increase in plastic area.

The plastic contact area will then be

$$A_p = n \eta \beta \sigma \pi \int_{h+\alpha_p}^{\infty} (s-h) \Phi^*(s) ds$$

$$\alpha_p^* = \frac{\alpha_p}{\sigma} \approx \frac{\beta}{\sigma} \left(\frac{H}{E'} \right)^2$$

Greenwood chooses $\Psi = \frac{E'}{H} \sqrt{\frac{\sigma}{\beta}}$ as the index of plasticity and determines two critical values by numerical resolution:

Ψ	0.6		1
nature of contact	elastic at the level of asperities themselves at high loads		plastic at the level of asperities themselves at low loads

This model proposes then a study of contact of a rough plane and a polished plane for surfaces satisfying the static condition of ergodicity, that is to say without texture, which is never the case for surfaces obtained during classical machining. A rectified surface, for example, will show very different profilometric lifting according to the handling directions (parallel or perpendicular to the rectification stripes). The ideal surfaces for application of this model will be sanded surfaces. /51

The index of plasticity previously defined is not valid for a study of contact between a rough surface and an ideally polished plane. If the two surfaces are rough, one can have an estimate of contact behavior according to the index of plasticity [28] taking for the curve of asperities, the total of the curves of contact asperities $\frac{1}{\beta} = \frac{1}{\beta_1} + \frac{1}{\beta_2}$ and as the typical variation $\sigma = \sqrt{\sigma_1^2 + \sigma_2^2}$

A II: GREENWOOD AND TRIPP MODELS /52

If the apparent contact area is limited due to curvature of the body, which is often the case mechanically, the discrete contacts will no longer be independent, the compliance at one asperity depending on compliance at a neighboring asperity, The preceding model is incomplete therefore.

Let us consider contact of a smooth ball with diameter 2B on a rough plane, under load P (figure A4).

Equations (4), (5), (6) are always valid but u depends on r, the distance from the asperity to the axis of the ball.

$$N = \eta a F_0\left(\frac{u(r)}{\sigma}\right)$$

$$A = \eta n a \beta \sigma F_1\left(\frac{u(r)}{\sigma}\right)$$

$$P = \frac{4}{3} E' \beta^{1/2} \eta a \sigma^{3/2} F_{3/2}\left(\frac{u(r)}{\sigma}\right)$$

If one assumes that the load P, divided locally into nominal area, is conducted at a uniform pressure $\frac{P}{a}$, the distribution of pressure in the apparent contact area will be:

$$p = \frac{P}{a} = \lambda F_{3/2}\left(\frac{u(r)}{\sigma}\right)$$

with $$\lambda = \frac{4}{3} \eta E' \beta^{1/2} \sigma^{3/2}$$

It is then necessary to know the relationship between separation u and radial position r.

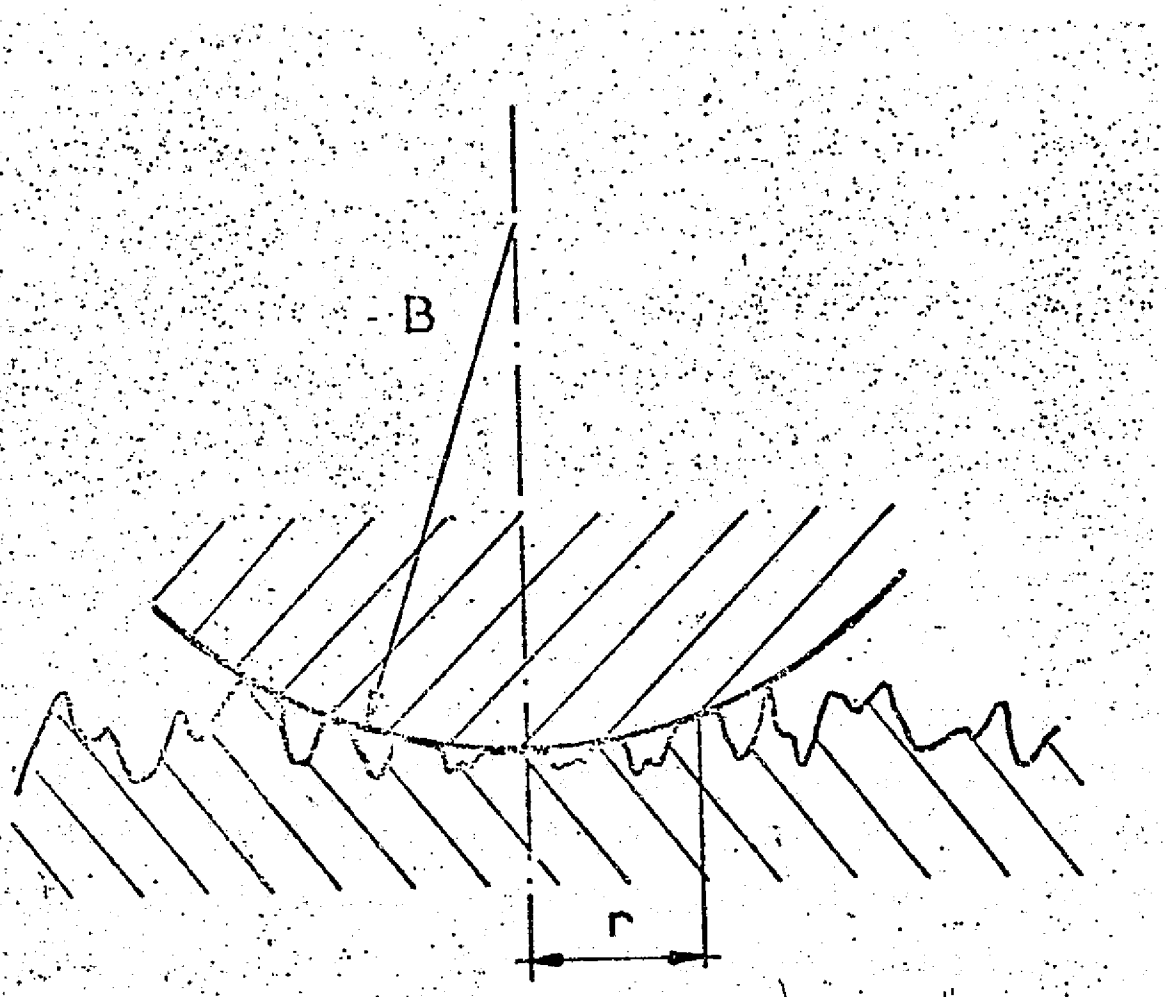

FIGURE A.4

For this type of smooth ball and rough plane contact, /54

$$u(r) = d + \frac{r^2}{2B} + w(r) - w(o)$$

where d is the separation between the nominal surfaces at the center of the ball, w(r) the elastic deformation at radial position r, w(0), elastic deformation at the center of contact.

from which $$p(r) = \lambda F_{3/2}\left[\frac{1}{\sigma}\left(d + \frac{r^2}{2B} + w(r) - w(o)\right)\right]$$

w(r) and w(0) are data from the theory of elasticity [11], figure A5

$$w(r) = \frac{4(1-\nu^2)qa}{\pi E}\int_0^{\frac{\pi}{2}} \sqrt{1 - \frac{r^2}{a^2}\sin^2\psi}\, d\psi$$

for $o \ll r \ll a$

$$w(r) = \frac{4(1-\nu^2)qa}{\pi E}\left[\int_0^{\frac{\pi}{2}} \sqrt{1 - \frac{a^2}{r^2}\sin^2\theta}\, d\theta - \left(1 - \frac{a^2}{r^2}\right)\int_0^{\frac{\pi}{2}} \frac{d\theta}{\sqrt{1 - \frac{a^2}{r^2}\sin^2\theta}}\right]$$

for $a \leq r \leq \infty$

This equation solved by Greenwood thanks to treatment on a computer leads to the following results:

- At low loads, the mean pressure in the apparent contact area is lower than that obtained for a polished body and the apparent contact area is larger.

- At high loads, the distribution of the pressures approaches Hertzian distribution (figure A6). Greenwood and Tripp, thus extend to rough bodies the problem of contact between a polished body initially solved by Hertz [11]. The roughness model assumes N asperities per unit of surface, the same curvature radius β in which the peaks follow the distribution of Gaussian heights characterized by σ for its variation type. Figure A7 summarizes their conclusions.

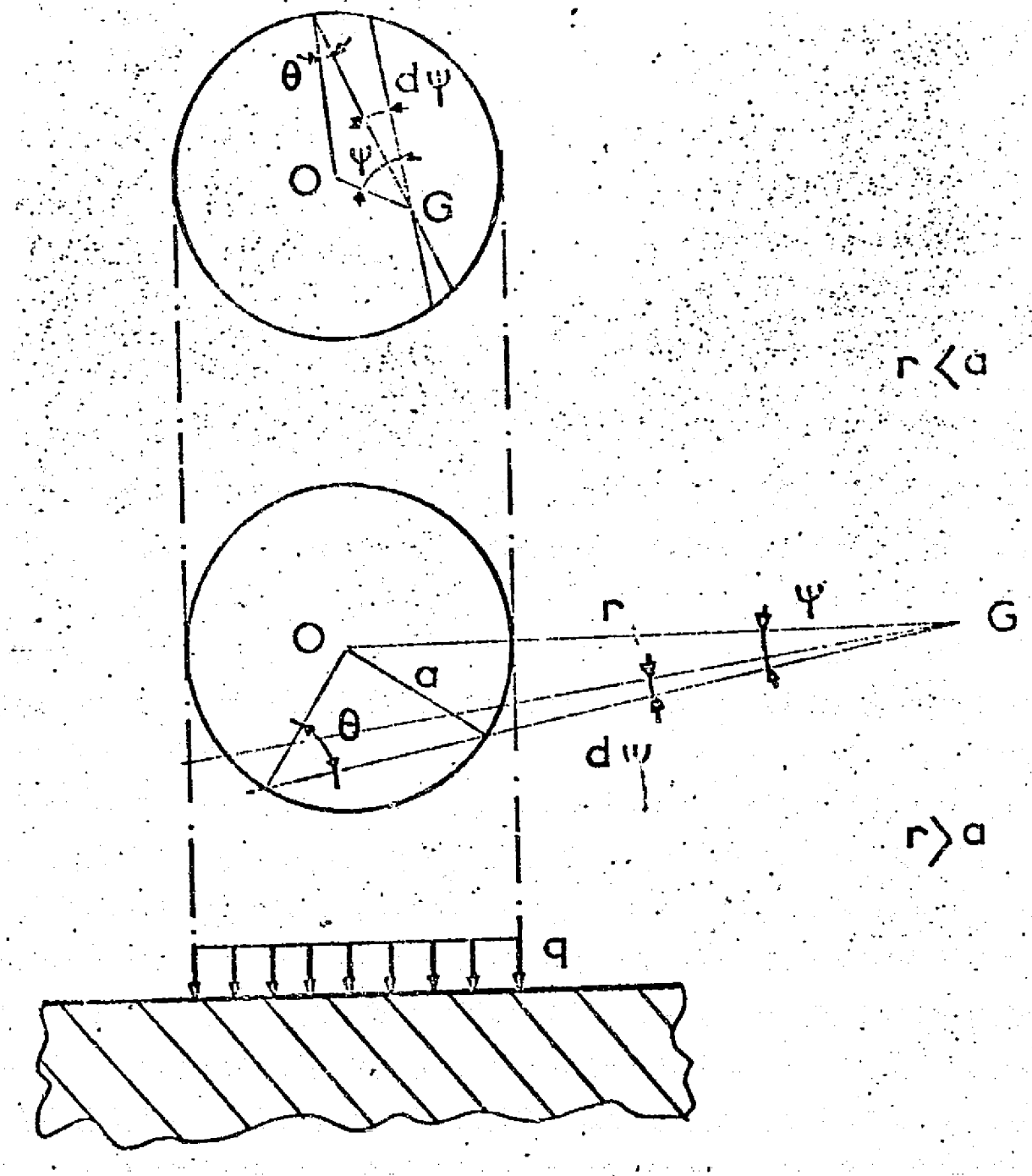

FIGURE A.5

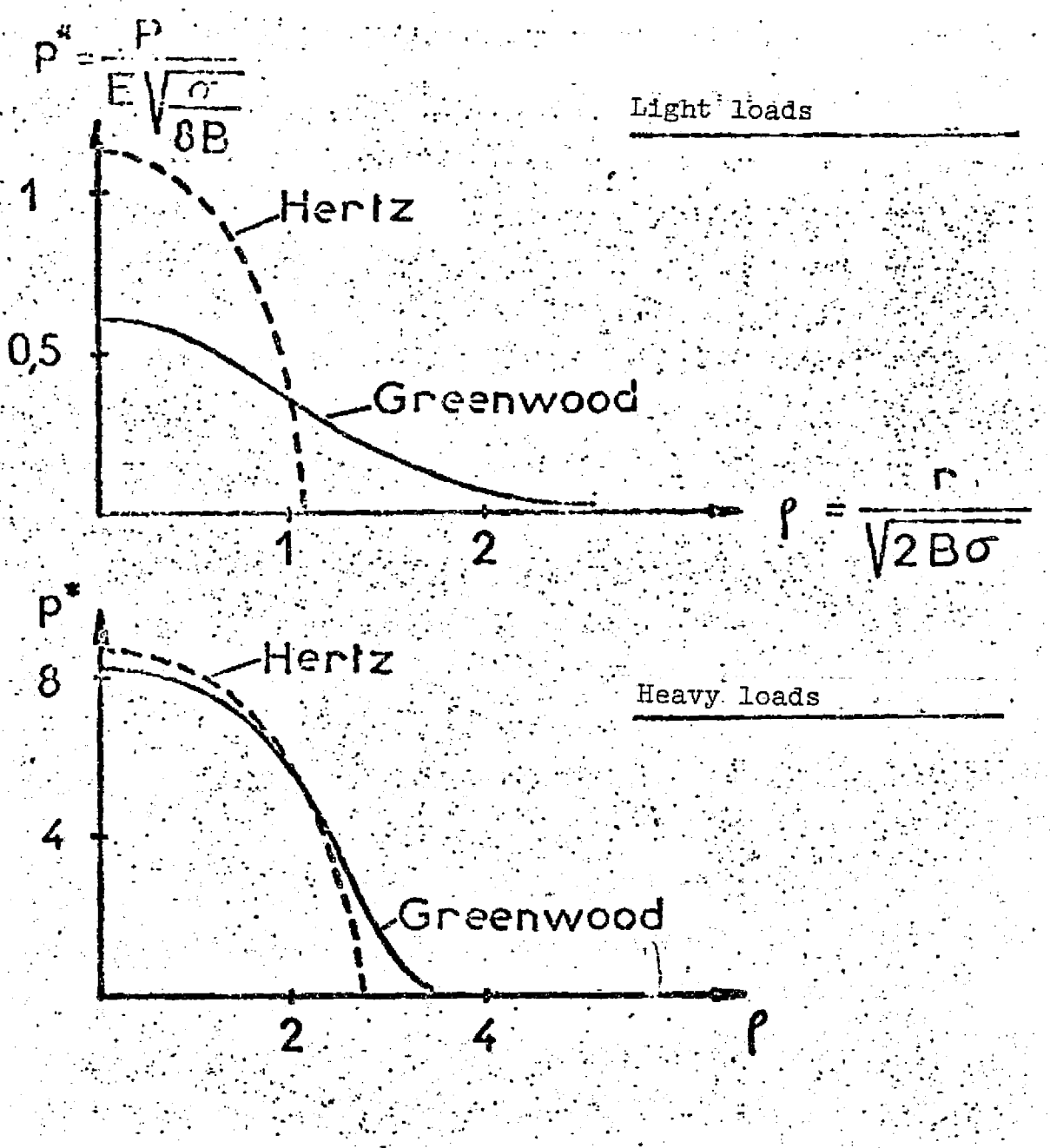

p^*, ρ : pressure and radial distance in adimensional variables

FIGURE A.6

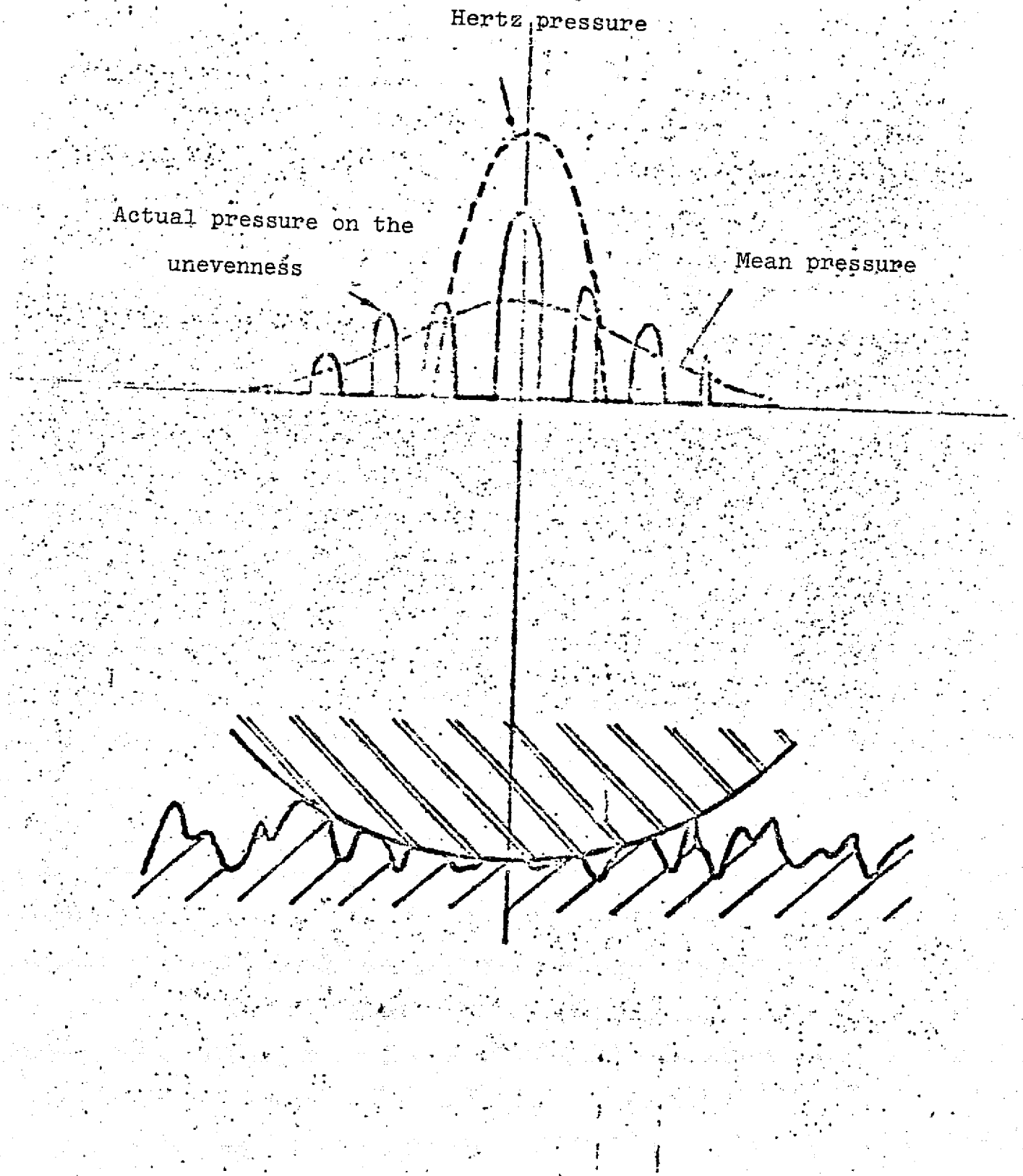
Hertz pressure
Actual pressure on the
unevenness
Mean pressure

FIGURE A.7

A III: WHITEHOUSE, ARCHARD AND ONIONS MODELS /58

The profile of the surface is considered as an aleatoric sign and is characterized by two functions used in treating the sign:

- The distribution of ordinatesof the profile, Gaussian (figure A8)
- The function of autocorrelation or its Fourier transform, spectral power density (figure A9)

Experiments have shown [29] that the function of autocorrelation is exponential for most of the surface profiles:

The profile then will be defined by two functions:

$$f(y) = \frac{1}{\sqrt{2\pi}} e^{-y^2/2} \qquad C(\beta) = e^{-\beta/\beta^*}$$ figure (A8,9

Two parameters will characterize the surface profile:

- σ^* variation type of distribution of profile ordinates.
- $\ell = 2.3\beta^*$ length of the correlation, knowing the distance from which two events of the profile can be considered independent (CCβ valued at 0.1 for $\beta = 2.3\beta^*$)

Archard and Onions [26], with this model, have developed a study of contact of rough planes, and a polished plane like that done by Greenwood and Williamson [1]. We will not reproduce their calculations but will limit ourselves to a comparison of the two models:

- Power spectral density shows us that there is a spectrum of defects of different sizes on the profile of one surface.
- Like the model of Greenwoodand Williamson, Whitehouse and Archard use a Gaussian distribution for profile ordinates.
- Whitehouse and Onions define the mean wavelength of surface defects related to β^* showing the exponential function of autocorrelation and, the asperities being assumed spherical, end in a calculation of mean curvature radius

$$R = \frac{(2.3\beta^*)^2 \cdot 2\sqrt{\pi}}{9\sigma}$$

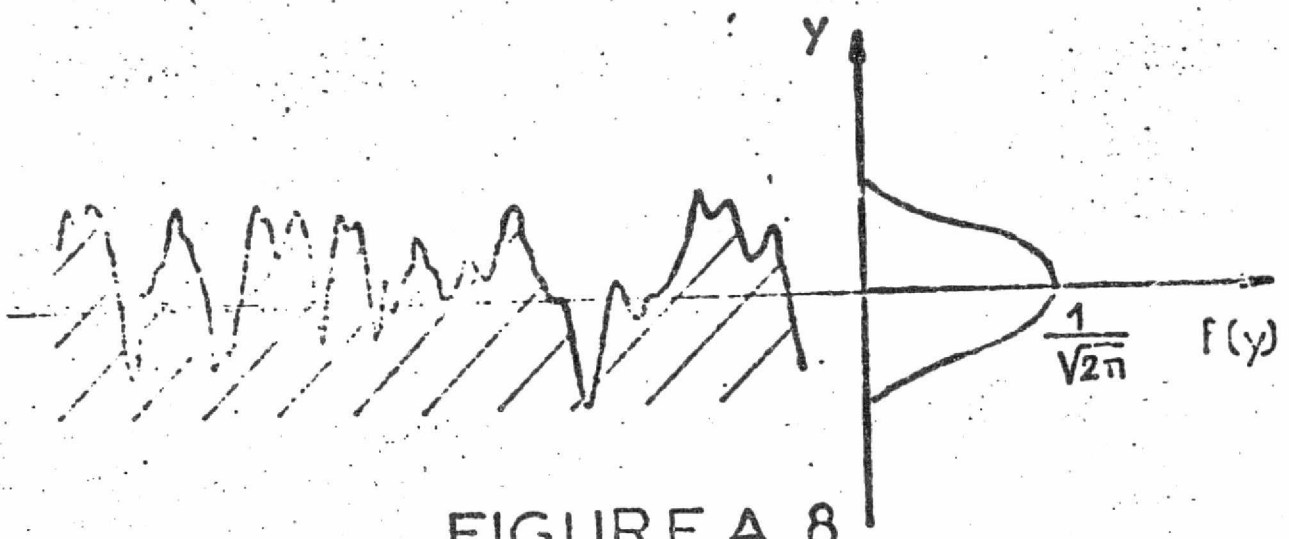

FIGURE A.8

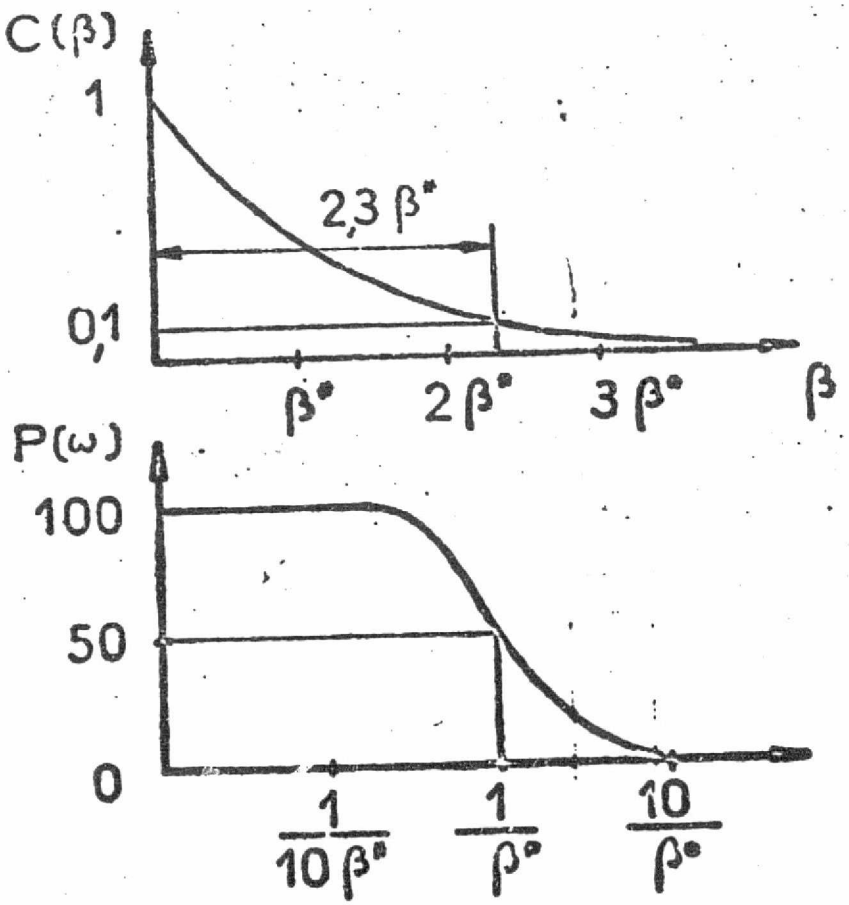

FIGURE A.9

- According to the Greenwood model, a profile is characterized by three parameters σ, β, N; Whitehouse and Archard characterize the profile with two parameters σ^* and β^*, the curvature radius and the number of surface defects being related to the mean wavelength of surface defects. /60

- Whitehouse and Archard define the index of plasticity which is given the same significance as that of Greenwood

$$\Psi = \frac{E'}{H} \cdot \frac{\sigma^*}{\beta^*}$$

A IV: BALANCE SHEET OF THE ANALYSIS METHOD USED /61

Besides the study of the two contact types, a polished plane and rough plane, the smooth ball bearing and the rough plane, these models suggest to us a precise microgeometric characterization of the surface states. These known quantities, σ, β, N, σ^*, β^*, deduced from digital analysis of profilometric summaries do not evidently characterize any surface except one whose condition is ergodic, that is to say, if the profiles obtained lead to the same statistical known quantities as that of the direction of handling chosen for the surface (for example, for standard surfaces).

Experimental Method Used

A Talysurf 4 Taylor Hobson roughness meter makes it possible to obtain the electrical image of a sample studied using an electrodynamic sensor. This electrical signal is then amplified with the possibility of filtering it. It is derived equally and a logic system delivers a pulse to each pass at zero of the derivative which makes it possible to use the maxima or minima of the signal in the series of samples.

The electrical signal obtained is then treated in two different ways:

- The first consists of a statistical analysis which is carried out in real time using a Hewlett Packard correlator, model 3721A. This makes it possible for us to study the ordinates of the profile and the profile maxima which leads to functions of distribution and autocorrelation.

- The second consists of a frequency analysis also carried out in real time using a Spectral Dynamics SD 301 B analyzer which makes it possible to attain the power spectral density curves.

The diagram of our range of measurement is recorded in figure A10. Figures A11 and A12 give the results obtained for one of the sandedc samples used during a boundary friction test.

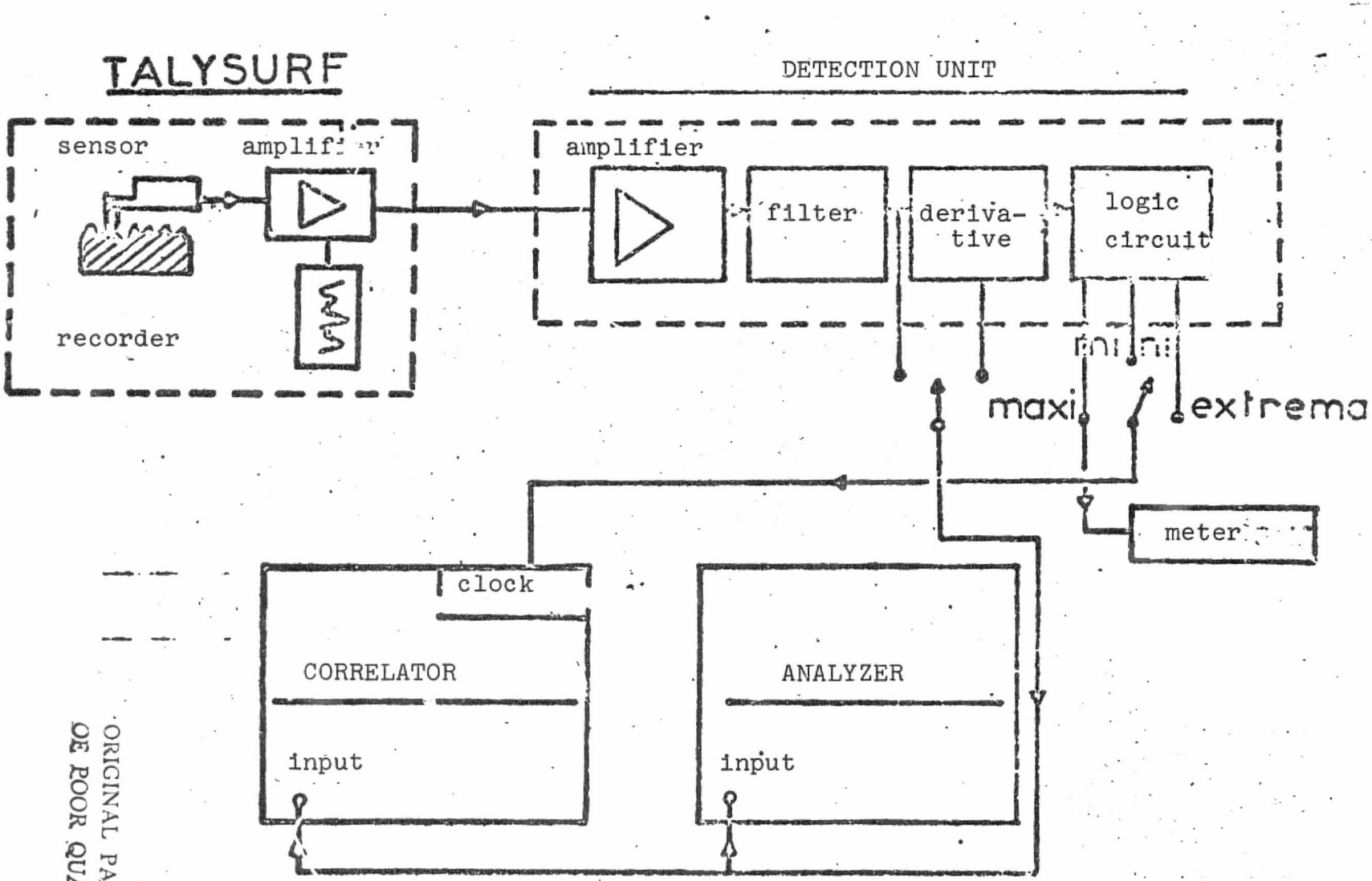

FIGURE A.10

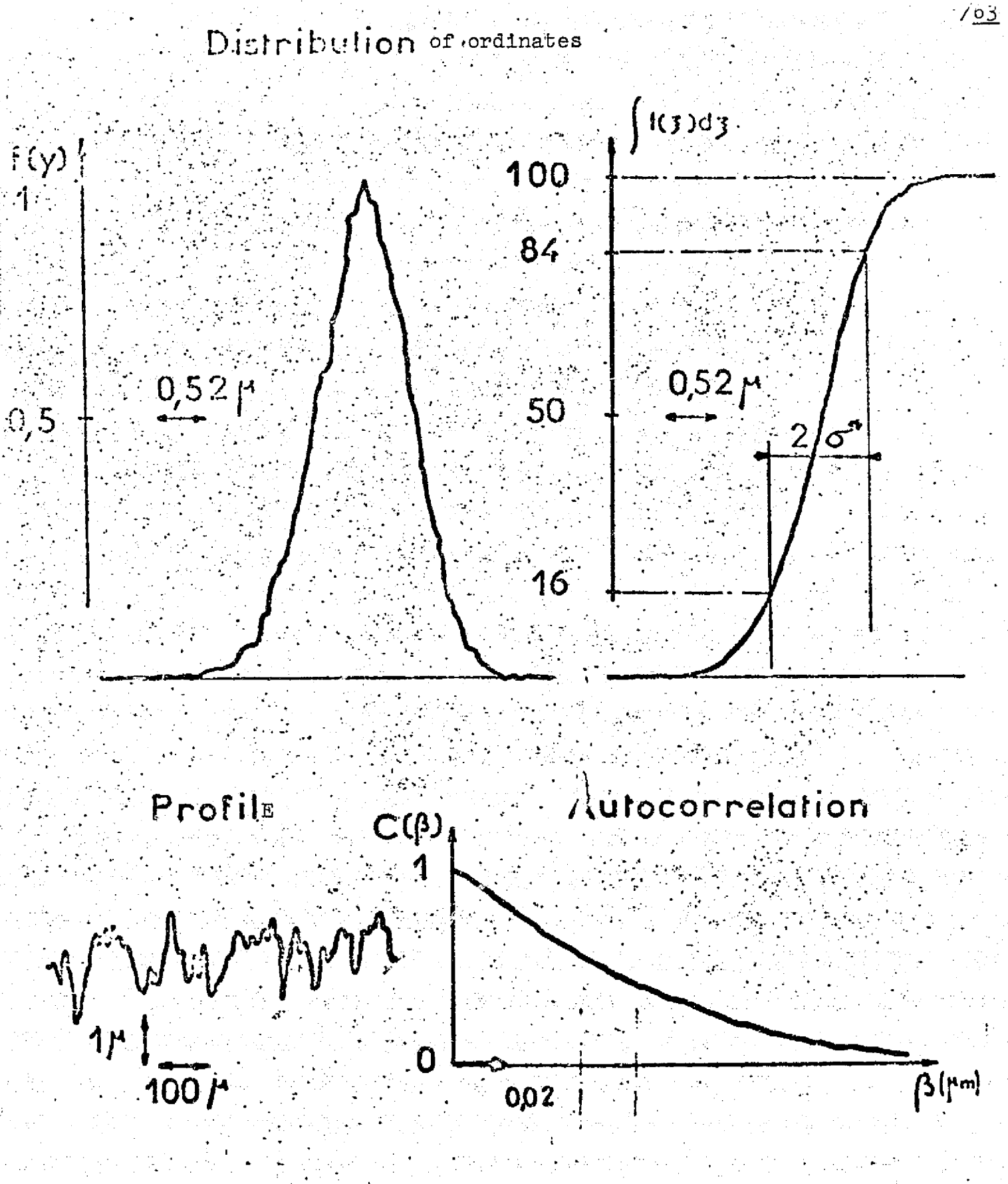
Distribution of ordinates
f(y)
1
0,5
0,52 μ
∫f(z)dz
100
84
50
16
0,52 μ
2 σ
Profile
1μ
100 μ
Autocorrelation
C(β)
1
0
0,02
β(μm)

FIGURE A.11

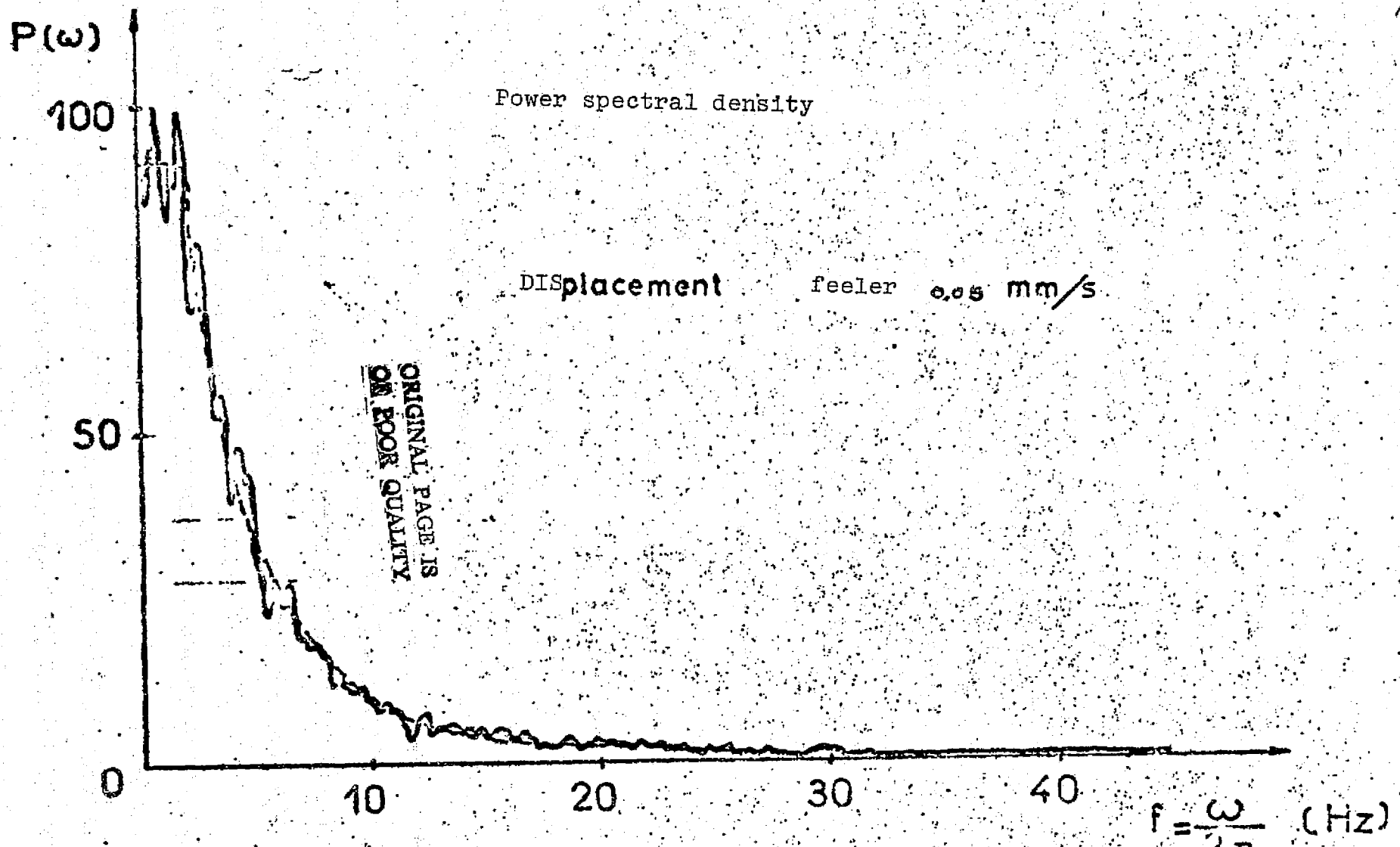

FIGURE A.12

APPENDIX B

/65

STATIC CONTACT WITH FORCE

TANGENTIAL CONTACT IN MOTION

BI Static Contact with Tangential Force

- Dry Contact without the Intervention of a Lubricating Film

The Theoretical Model in Two Dimensions [30]

The Von Mises outflow criterion, as an orthonorm reference mark, is written for the Cartesian coordinates.

$$\frac{1}{2}\left[(\sigma_x-\sigma_y)^2+(\sigma_y-\sigma_z)^2+(\sigma_z-\sigma_x)^2+6\left(\tau_{yz}^2+\tau_{zx}^2+\tau_{xy}^2\right)\right]=3k^2$$

Let us consider the case of a theoretical model in two dimensions (figure B1). A block of soft metal is pressed against a hard plane under normal pressure σ and is subjected to equivalent tangential action at shear constraint s, in such a way that the shearing appears in the ABCD zone. As it is impossible to having shearing the length of surfaces AD and BC, the shear constraint the length of CD must be cancelled by C and D. In order to equalize the pair existing in the ABCD zone, in a simple manner, the constraints are assumed [30] to have a constant value the length of AD and CB.

The outflow equation is reduced in this case to:

$$\sigma^2+3s^2=3k^2$$

but $\gamma = k\sqrt{3}$, γ being the critical constraint of stress in pure traction. In effect, in pure traction, $\sigma_4 = \gamma$ $\sigma_2 = \sigma_3 = 0$, σ_4 σ_2 σ_3 are the principal components of constraint and the Von Mises criterion which is expressed as a function of these principal components by:

$$\frac{1}{2}\left[(\sigma_1-\sigma_2)^2+(\sigma_2-\sigma_3)^2+(\sigma_3-\sigma_1)^2\right]=3k^2$$

then gives $\gamma=\sqrt{3}k$

The outflow equation becomes:

$$\sigma^2+3s^2=\gamma^2$$

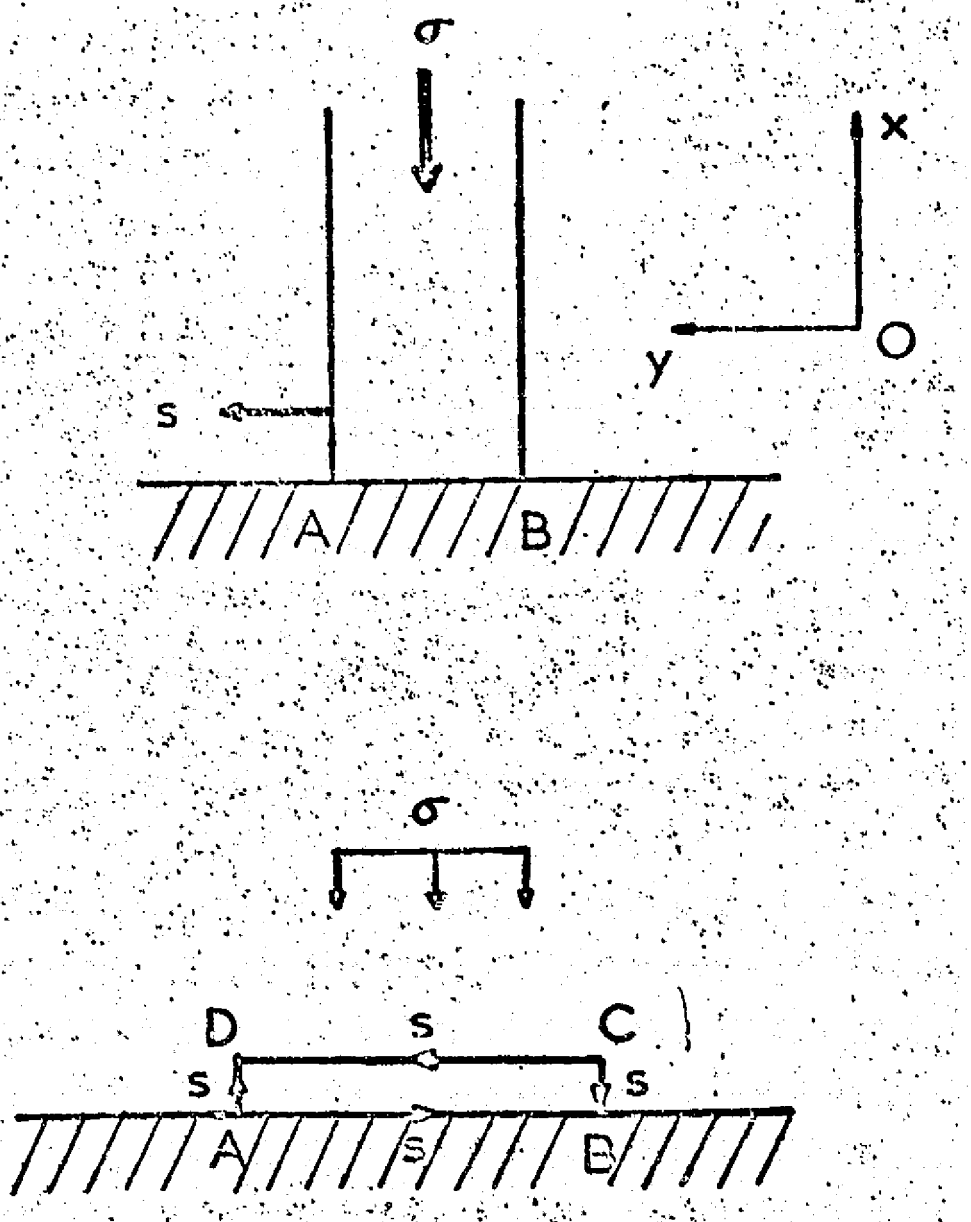

FIGURE B.1

Actual Model /67

If one applies pure compression, the theoretical model above gives us $\sigma = Y$. But an actual surface will have plasticized asperities for very low loads and the normal constraint will become equal to the critical pressure, equal at 3Y during totally plasticized contact.

By adding a shear tangential constraint, the relationship among σ, s, Y becomes very complex and Tabor [30] assumes that it must have the form:

$$\alpha \sigma^2 + \beta s^2 = \gamma Y^2$$

α, β, γ being the numerical coefficients.

It has been shown [31] that when two bodies are subjected to a normal course then to a tangential force, there is a plastic outflow and an increase in the contact area of the junctions which accompanies microdisplacements of one body in relation to another.

If one considers two bodies in ideal contact following a single junction, a normal load W produces contact area Ao. Under the effect of tangential force F, the contact area increases to A. The initial pressure $p = \frac{W}{A_o}$ becomes $p = \frac{W}{A}$ and the tangential constraint is $s = \frac{F}{A}$.

The outflow criterion will be: $p^2 + \alpha s^2 = p_o^2$

For a problem of two dimensions, Tabor [30] has shown that $\alpha = 3$ and has chosen in the case of actual contact [30], $\alpha = 9$ which results in

$$p^2 + 9s^2 = p_o^2$$

Other values, notably $\alpha = 12$, have been proposed [32].

If p tends towards zero, the shear constraint s becomes sm, the critical shear constraint of the metal and one will have:

$$p_o^2 = 9\, sm^2$$

from which $p^2 + 9s^2 = 9\, sm^2$

- Contact with a Lubricant Film

The shear constraint si of the lubricant film is lower than the critical shear constraint sm of the metal. As long

as the shear constraint is lower than si, the tangential constraint transmitted to the underlying metal and plastic deformation is expressed by an increase in junctions under the combined effect of compression and shear constraint. As soon as the shear constraint becomes equal to si, the increase in junctions stops and one has shear at the interface film level. /68

The slip condition of the interface becomes:

$$p^2 + 9si^2 = 9\,sm^2$$

Whether or not there is a lubricating film, applying progressive contact constraint causes plastic deformations which are expressed by preliminary displacement [33], an increase in the junctions, a compression of the metal in front of the friction piece [14].

These phenomena are very important because they are initiators of the contact slip process, the friction piece having then the role of shearing the deformed metal at the interface (figure 2.1) or of compressing it [14].

B II Contact in Motion

As was verified in the first section of this text, the motion contact will be characterized, according to mechanical, geometrical and chemical conditions by a plowing and shearing interface or by a softer deformation.

Kragelsky [25] has shown, by an experiment of a friction piece on a plate, how the passage of a "soft" friction piece to a "hard" friction piece was related to physical characteristics of contact (figure B2). At low loads, the frontal protrusion of the material pushed back in front of the friction piece during preliminary displacement is pushed back without tearing, being pared and sheared when the load becomes more important.

These deformation models, mainly qualitative, which illustrate the motion contact in the case of ideal contact are very useful for understanding the phenomena located in an interface, notably during conditions of boundary lubrication.

- Bowden and Tabor [34] propose a theory other than that of deformation. They propose a double formula for friction resistance, the first term being due to displacements of plastically deformed metal and the second due to adhesion.

/69

Ball bearing: steel

Block: checkered plasticine

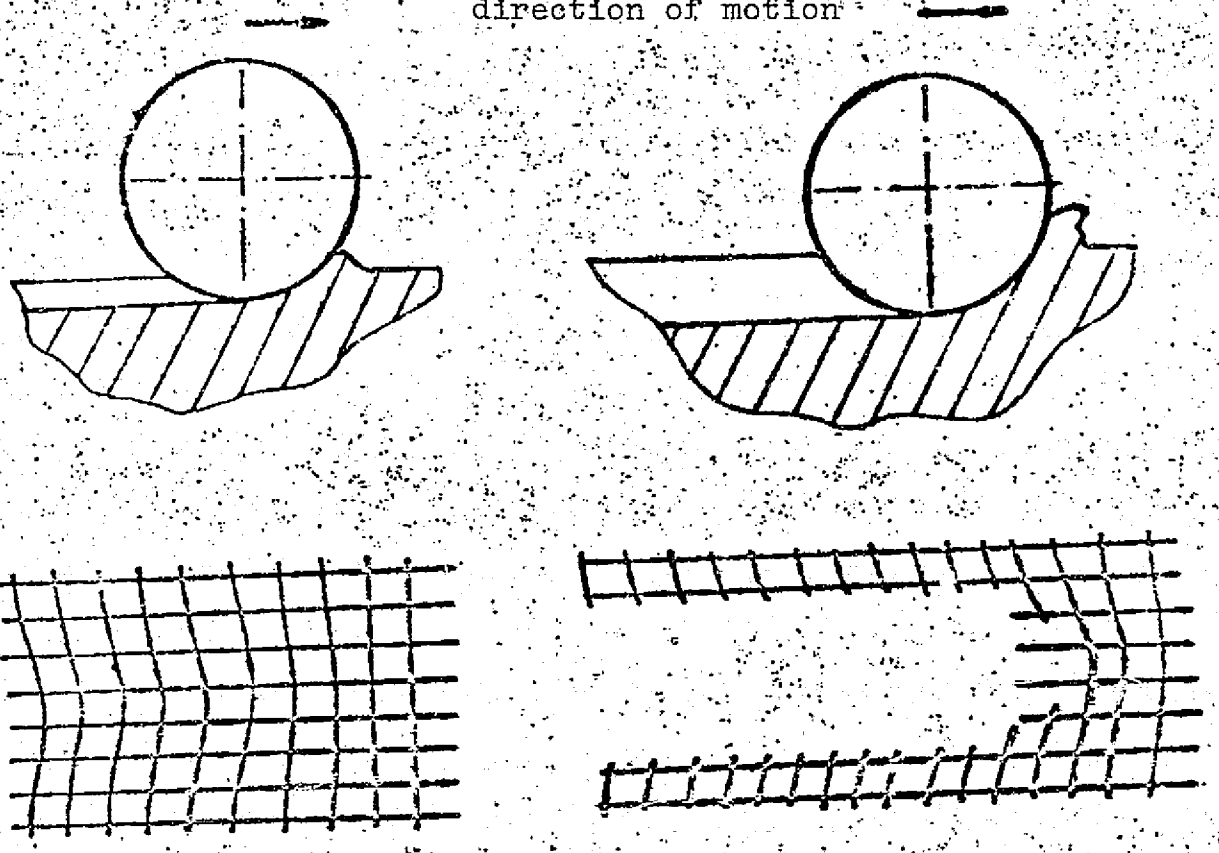

Frontal protrusion pushed back without tearing

Shearing of frontal protrustion

FIGURE D.2

$$F = F_1 + F_2 \rightarrow \text{due to paring of the metal}$$
$$\downarrow$$
due to adhesion

They consider that the adhesion term is predominant.

from which $F = F_1 = A\ s \rightarrow$ shear constraint of the interface /70

$\downarrow$ Actual contact area

The friction coefficient is $f = \frac{F}{W}$

but $W = AH$ hardness

from which $f = \frac{As}{AH}$, $f = \frac{s}{H}$

The friction coefficient was then uniquely dependent upon physical characteristics of the contact materials.

This model based upon adhesion theories was subject to criticism due to practical considerations. During the friction test, the metal transferred by adhesion is very slight in relation to that which these theories predict [35]. It was also suggested by [36] that the slip rate must be an important factor.

The laws of friction regulate contact at very low rates being related to diffusion phenomena, adhesion seen throughout as important as a junction. At higher rates, the time available for action of these processes is reduced more and the coefficient of friction decreases.

These two approaches by adhesion and deformation must be complementary; the relative importance of one to the other can depend on the type of contact studied.

/71

APPENDIX C

EXAMPLES OF EXPERIMENTAL SUMMARIES Rc = f(W)

fig C.1	Polished friction piece Rough plate	3 Films
fig C.2	Polished friction piece ASB Film	3 Roughnesses
fig C.3	Polished friction piece CB Film	2 Hardnesses
fig C.4	Polished friction piece ASB Film	2 Hardnesses
fig C.5	Polished friction piece Ethyl laurate	3 Hardnesses

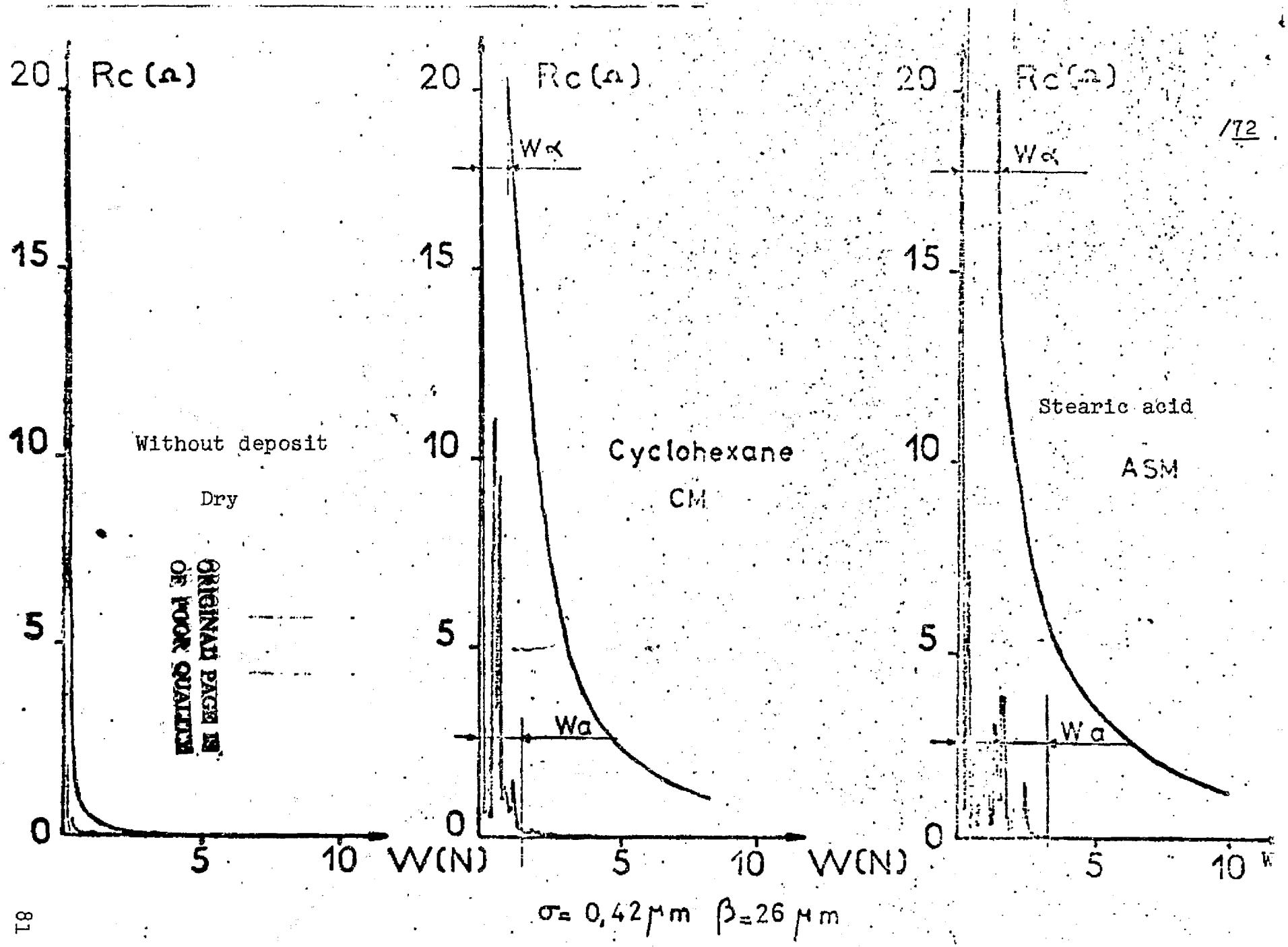

FIGURE C.1

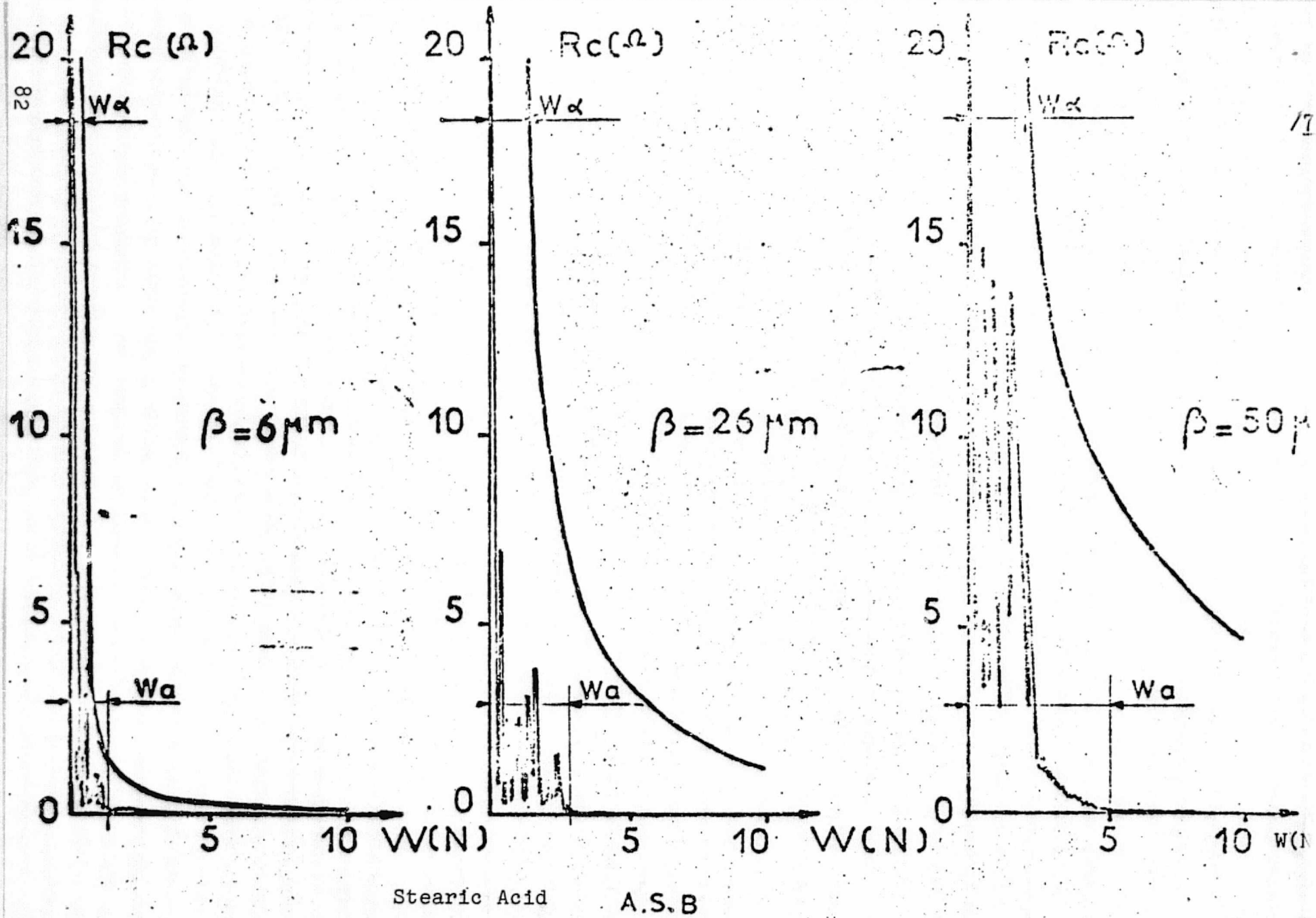

Stearic Acid A.S.B

FIGURE C.2

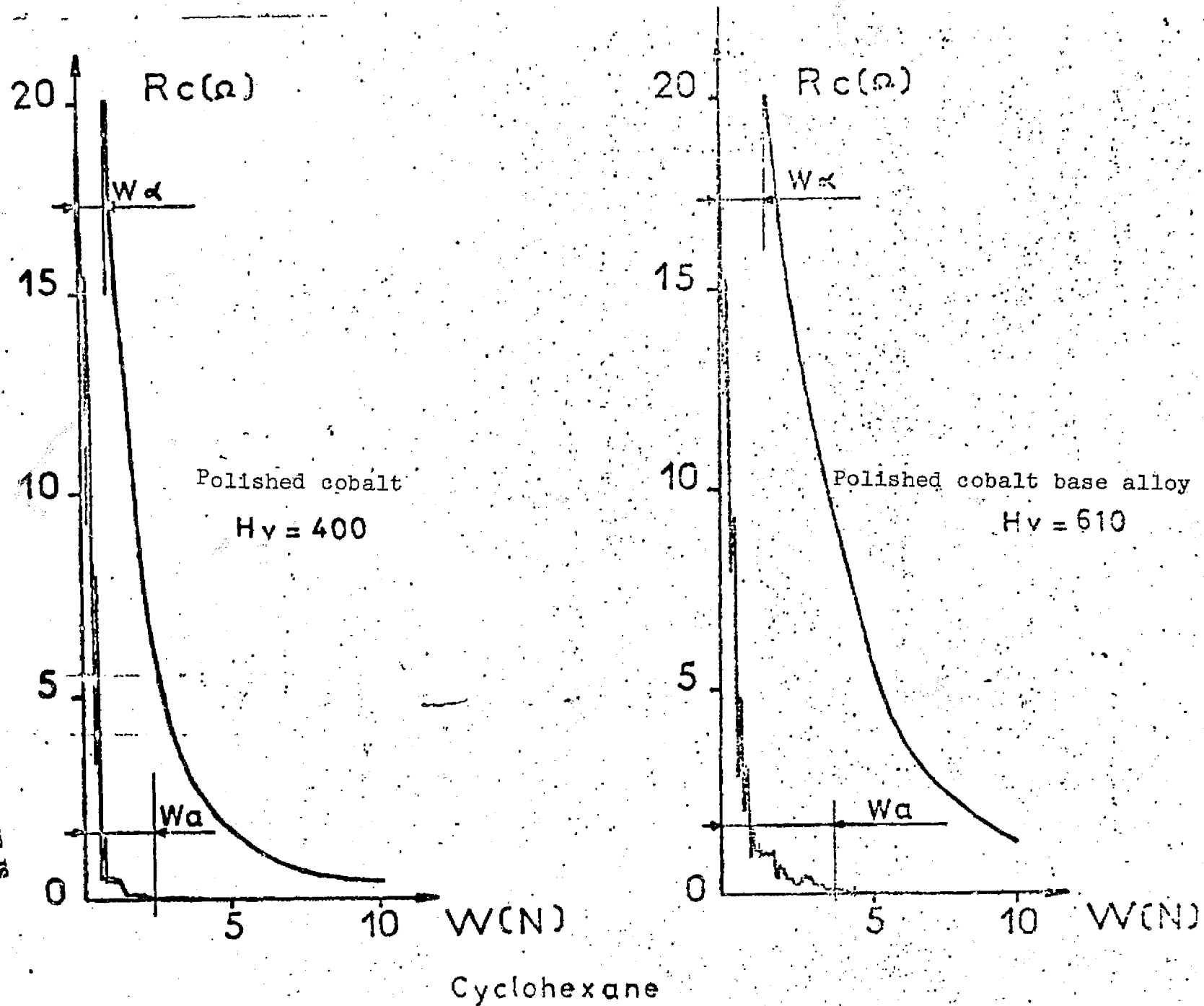

FIGURE C.3

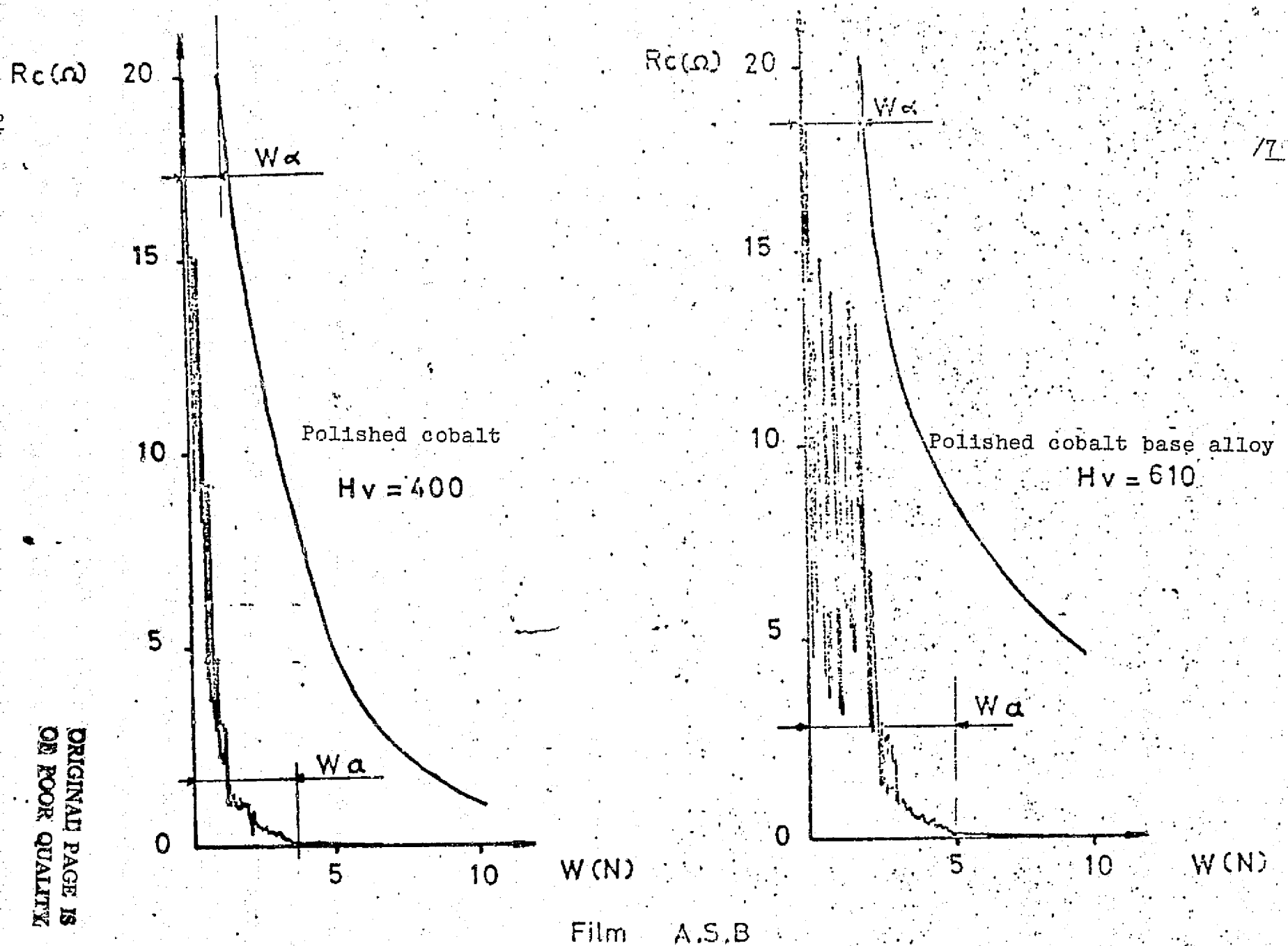

Film A.S.B

FIGURE C. 4

SAMPLE	1	2	3
Wa MEAN (N)	12	10	8
HARDNESS Hv	820	610	200

Figure C.5

- friction piece: polished cobalt base alloy
- plates: 100 C6 steel austenized 30 min at 825°C oil tempering
  - sample 1: tempering 1 hr at 180°C
  - sample 2: tempering 1 hr at 350°C
  - sample 3: annealed state
- film: ethyl laurate

REFERENCES

1. Greenwood,, J.A. and J.B.R. Williamson, Proc. R. Soc., London A295, 300-319 (1966).

2. Whitehouse, D.J. and J.F. Archard, Proc. R. Soc., London A316, 97-121 (1970).

3. Brocknay, L.O. and R.L. Jones, Advan. chem. 43, 275 (1964).

4. Rosterin, J.I. and I.V. Kragkelsky, Friction and wear in machinery, V. 12, 19[illegible] p. 111.

5. Holm, R., Electric cont[illegible]cts, Springer Verlag, Berlin, 4th edition, 1967, p. 125.

6. Hirst, W., Kerridge, M. and J.K. Lancaster, Proc. R. Soc., London A212, 516-520 (1952).

7. Zisman, W.A., Friction and wear, Ed. R. Davies, Elsevier, 1959, pp. 110-148.

8. Bigelow, W.C., Pickett, D.L. and W.A. Zisman, J. Colloid. Sci. 1, 513 (1946).

9. Blodgett, K.B. and I. Langmuir, Phys. Rev. 51, 964 (1937).

10. Woog, P., Contribut[illegible]n [illegible] l'étude du graissage [Contribution to the study of lubrica[illegible]on], Delagrave, Paris, 1926.

11. Timoshenko, S. and J.N. [illegible]odier, Theory [illegible]sticity, McGraw Hill Book Co., Inc., New York, N.[illegible]., [illegible]51.

12. Tabor, D., The hardness of the metals, Oxfo[illegible]larendon Press, 1951.

13. Greenwood, J.A. and J.H. Tripp, Proc. Inst. Mech. Engrs. 185, 625 (1970-71).

14. Courtel, R., C.R. Ac. Sc. 253, (1961), 261, (1965).

15. Tabor, D., and R.F. Willis, Wear 13, 413-442 (1969).

16. Chilabra, D.S. and G.T. Wenning, Proc. Electrical Contacts, (1965).

17. Georges, JM. and T. Mathia, In preparation.

18. Greenwood, J.A., Trans. ASME F 89, 81 (1967).

19. Bowder, F.P. and D. Tabor, The friction and lubrication of solids, Part I, Clarendon Press, Oxford, England, 1971, p. 16.

20. Fein, R.S., Lubrication 57/1, (1971).

21. Scrutton, B, Tabor, D. and R.F. Willis, Nature 236, 65 (1972)

22. Holm, R., Electric contacts, Springer Verlag, 4th edition, Berlin, 1967, p. 43.

23. McFarland, J.S. and D. Tabor, Proc. Roy. Soc. A202, 244 (1956).

24. Courtel, R., Met. Corrosion Ind. 473, 1-6 (1965).

25. Kragelskii, I.V., Friction and wear, Butterworths, London.

26. Onions, R.A. and J.F. Archard, J. Appl. Phys. 6 (1973).

27. Tabor, D., The hardness of the metals, Oxford Clarendon Press, 1951.

28. Greenwood, J.A. on discussion of E.A. Wilson. Journal of Lubrication Technology, Trans. ASME F 89, 521-522.

29. Peklenik, Proc. Inst. Mech. Engrs. 182, 108 (1968).

30. Bowden, F.P. and D. Tabor, The friction and lubrication of solids, Part I, Clarendon Press, Oxford, England, 1971, p. 102.

31. Tabor, D., Proc. Roy. Soc. 251, 378-393 (1959).

32. Courtney-Pratt, J.S. and E. Eisner, Proc. Roy. Soc. A238, 529-550 (1957).

33. Bailey, J.M. and A.T. Gwatmey, A.S.L.E. Trans. 5/1, (1962).

34. Tabor, D., Surface and colloid Science 5, 245 (1972).

35. Bikerman, J.J., J. Appl. Phys. 30/3, 448-449 (1959).

36. Ling, F.F. and E. Saibel, Wear 1/3, 167-172 (1957-58).